UC-34d
UC-4

Submitted to Physical Review

LBL-6984 c.1
Preprint

NMR DOUBLE QUANTUM SPIN DECOUPLING IN SOLIDS

A. Pines, S. Vega, and M. Mehring

October 1977

Prepared for the U. S. Department of Energy
under Contract W-7405-ENG-48

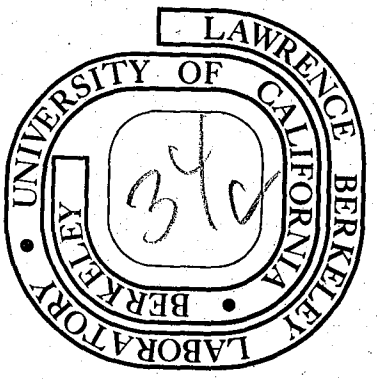

LBL-6984

NMR Double Quantum Spin Decoupling in Solids

A. Pines, S. Vega[†] and M. Mehring[‡]

Department of Chemistry
University of California
Berkeley, CA 94720

ABSTRACT

The problem of spin decoupling spin I=1 nuclei with large quadrupolar splittings ω_Q (e.g. deuterium) from dilute S spins via double quantum transitions is dealt with. The normal two spin-½ single quantum decoupling problem ($I=\frac{1}{2}, S=\frac{1}{2}$) is first dealt with as a reminder of the coherent averaging approach and to understand the dependence of the S resonance linewidth on the I rf field intensity (ω_1) and resonance offset ($\Delta\omega$). The double quantum problem ($I=1, S=\frac{1}{2}$) is then treated analogously by introducting fictitious spin-½ operators for the I double quantum transition. The decoupling condition is found to be very sensitive to the spin-I resonance condition and to go as $\sim \frac{1}{\omega_1^4}$ with the spin I rf field intensity at resonance in the double quantum regime ($\omega_1 << \omega_Q$). Experimental examples on heavy ice, dimethyl-sulfoxide-d_6 and benzene-d_6 are presented verifying the quantitative theoretical predictions. Extensions to higher order multiple quantum effects for spin I > 1 and for several coupled spin-½ nuclei are discussed.

I. INTRODUCTION

The application of heteronuclear spin decoupling has made an important contribution to solid state nmr. In its most common form we have a sample with abundant spins I and dilute spins S. By strongly irradiating the I spins with a radio frequency field near their Larmor frequency we can spin decouple them from the S spins[1] allowing the observation of a high resolution spectrum. Figure 1 depicts this approach in simple schematic terms, showing the S free induction decay while continuously irradiating the I spins. This has been applied to nmr of ^{13}C and other nuclei in solids.[2]

A potentially useful candidate for such experiments is the case I ≡ deuterium, S ≡ proton. By spin decoupling the deuterium in a $\gtrsim$ 99% deuterated sample we could directly observe a high resolution proton spectrum. Figure 2 indicates the difficulty of such an approach. The deuterium nucleus has spin-1 and the interaction of the quadrupole moment with electric field gradients causes a splitting of the spectrum into lines (two allowed transitions) separated by $2\omega_Q$, where ω_Q denotes a quadrupolar frequency. Typically, the splitting can be high, $\nu_Q \equiv \frac{\omega_Q}{2\pi} \sim$ 100 kHz. Thus, it might appear that the deuterium decoupling rf field intensity must be sufficient to cover the entire quadrupolar spectrum, i.e.,

$$\omega_1 \gtrsim \omega_Q \tag{1}$$

where ω_1 is the intensity of the rf field. The situation appears particularly acute in the case of a polycrystalline sample where all the orientations of the electric field gradients give a continuous distribution

of ω_Q. The deuterium nmr spectrum expected for such a case is shown in Figure 3 for an axially symmetric field gradient. Figure 4 shows an example of 99% deuterated dimethyl sulfoxide (DMSO-d_6) showing the center portion of such a spectrum. The maximum splitting is $2\nu_Q \approx$ 88 kHz which makes it difficult for our decoupling transmitter to cover the full spectral range.

It was realized a few years ago by Meiboom and co-workers[3] in their liquid crystal work that deuterium spin decoupling might take place via deuterium double quantum transitions, i.e., rapid transitions between the m = ±1 levels. Since the m=0 level does not affect the S spin this should indeed suffice. Furthermore, although this is a second order process it is resonant for all spins (the m = ±1 splitting is $2\omega_0$ independent of ω_Q to first order) and might provide a better mechanism for decoupling than the strongly off resonant allowed transitions. In fact, Meiboom et al. were able to decouple deuterium in oriented molecules in liquid crystal solution, where $2\omega_Q$ is a few kHz, with moderate rf fields. Very recently, we extended this to solids and showed that even in 99% deuterated ice where $2\omega_Q \sim 230$ kHz a field of $\nu_1 \equiv \frac{\omega_1}{2\pi} \sim 20$ kHz sufficed for spin decoupling.[4] Using second order perturbation theory, we estimated that instead of (1), the criterion for the onset of spin decoupling via double quantum transitions is actually much less stringent:

$$\omega_1 \gtrsim (\omega_Q D)^{\frac{1}{2}} \qquad (2)$$

where D roughly characterizes the I-S dipolar coupling.

Various schemes for deuterium spin decoupling have been proposed as indicated schematically in Figure 5. Except for special cases, the third approach of double quantum decoupling appears to be the simplest and has the most promise in terms of utilization of the rf power. The purpose of the present paper is to present a more quantitative analysis and set of experiments of spin decoupling for spin-1. We shall see that the result (2) is indeed borne out by a more rigorous analysis. The effects of frequency offset of the rf irradiation on the I-spins are also accounted for. The approach adopted is to calculate the effects of the quadrupolar and rf irradiation fields on the I-S dipolar coupling Hamiltonian $\mathcal{H}_{IS}$ and to find the conditions for making the effective $\mathcal{H}_{IS}$ vanish.

In Section II we outline the well known and simple problem of spin decoupling when both I and S are spins-½ so no quadrupolar splitting is involved. This serves to introduce the form of the Hamiltonian and to illustrate the approach for calculating the effective $\mathcal{H}_{IS}$ when rf irradiation is applied to the I spins, using coherent averaging theory.[5] This yields the expected condition for normal single quantum spin decoupling. The asymptotic dependence of the S linewidth on the I resonance offset and on ω_1 for large ω_1 is also estimated theoretically. In Section III the I-spin is taken as spin-1 with quadrupolar coupling parameter ω_Q. We introduce fictitious spin-½ operators used previously to describe double quantum coherence.[6] In the practically interesting case $D \ll \omega_1 \ll \omega_Q$ the system is formally identical to a fictitious spin-½ coupled to the S-spin and we derive the double quantum decoupling condition for the effective $\mathcal{H}_{IS}$. Again the asymptotic dependence of

the S-linewidth on ω_1 and $\Delta\nu$ is calculated.

In Section IV experimental results are presented illustrating the deuterium spin decoupling in solids and showing the behavior as a function of deuterium rf field ω_1 and resonance offset $\Delta\omega$ and comparison with theory. We conclude in Section V with an extension to two coupled spin-½ I spins where double quantum effects can also be observed and a brief discussion of higher order multiple quantum effects for spin $I = \frac{n}{2}$ or n coupled spins-½.

II. SPIN DECOUPLING FOR SPINS-½

This section is intended to serve as an introduction to notation and background for the subsequent application to the novel double quantum effects. The coherent averaging treatment for normal single quantum decoupling outlined here has been treated previously.[5]

A. Hamiltonian

The situation of interest here is depicted schematically in Figure 6. Spins I=½ interact with spins S=½ and are subjected to rf irradiation near their Larmor frequency and we neglect I-I and S-S couplings. The effects of many body I-I interactions have been treated elsewhere.[2c] We shall be interested in what follows in coherent I interactions due to quadrupolar couplings or a small number of dipolar interactions which lead to multiple quantum effects and where the calculation can be done exactly. Thus the neglect of many body I-I interactions is justified. This is especially so for 99% deuterated material, where the deuterium-deuterium coupling is not normally larger than deuterium-proton coupling, so the effects of I-I interactions on the spin decoupling are expected to be weak, and we need only to overcome the I-S interactions.[2c] We consider that I are abundant and S dilute, so several I spins interact with S of which only one is shown in Figure 6.

The spin Hamiltonian for this system in high magnetic field is given in angular velocity units by:

$$\mathcal{H} = -\omega_{0I} I_z - \omega_{0S} S_z - 2\omega_1 I_x \cos\omega t + \mathcal{H}_{IS} \qquad (3)$$

where ω_{0I} and ω_{0S} are the I and S Larmor frequencies, ω_1 is the intensity of the I rf field at frequency ω near ω_{0I} and $\mathcal{H}_{IS}$ is the truncated I-S dipolar interaction Hamiltonian:

$$\mathcal{H}_{IS} = S_z \sum_j b_j I_{jz} \tag{4}$$

The parameters b_j characterize the I-S dipolar coupling:

$$b_j = \frac{-2\gamma_I\gamma_S\hbar\, P_2(\cos\theta j)}{r_j^3} \tag{5}$$

where γ_I and γ_S are magnetogyric ratios, r_j is the distance between S and I spin j and θj is the angle between the S-I vector and the magnetic field.

In the rotating frame at frequency ω for I and ω_{0S} for S, (3) is transformed to:

$$\mathcal{H} = -\Delta\omega I_z - \omega_1 I_x + \mathcal{H}_{IS} \tag{6}$$

where

$$\Delta\omega = \omega_{0I} - \omega \tag{7}$$

and the counterotating rf terms have been ignored. We shall henceforth remain in the rotating frame.

B. Spin Decoupling Conditions

The Hamiltonian in (6) contains three terms; a resonance offset $\Delta\omega$, an rf field ω_1 and the I-S coupling. It is the third term $\mathcal{H}_{IS}$ which is responsible for the splitting and broadening of the S resonance.

We now calculate the effect of the first two terms on $\mathcal{H}_{IS}$ using coherent averaging theory.[5] This is done conveniently by applying a tilt (T) transformation to a new frame with the operator:

$$T_y = \exp(i\theta I_y) \tag{8}$$

such that the effective field in the rotating frame defined by $\Delta\omega$ and ω_1 is along the new z axis. The Hamiltonian in this tilted frame has the form:

$$\mathcal{H}' = -\omega_e I_z + \mathcal{H}'_{IS} \tag{9}$$

where:

$$\mathcal{H}'_{IS} = S_z \sum_j b_j \, (I_{jz} \cos\theta - I_{jx} \sin\theta) \tag{10}$$

and ω_e, θ are given by:

$$\omega_e = (\Delta\omega^2 + \omega_1^2)^{\frac{1}{2}} \tag{11}$$

$$\theta = \tan^{-1} \frac{\omega_1}{\Delta\omega} \tag{12}$$

We now calculate the effect of $\omega_e I_z$ on $\mathcal{H}'_{IS}$ assuming $\omega_e >> ||\mathcal{H}'_{IS}||$ by calculating the average I-S Hamiltonian $\bar{\mathcal{H}}'_{IS}$ due to coherent averaging by $\omega_e I_z$ at frequency ω_e:

$$\bar{\mathcal{H}}'_{IS} = \bar{\mathcal{H}}^{(0)}_{IS} + \bar{\mathcal{H}}^{(1)}_{IS} + \bar{\mathcal{H}}^{(2)}_{IS} + \ldots. \tag{13}$$

where:

$$\bar{\mathcal{H}}_{IS}^{(0)} = \frac{1}{t_c} \int_0^{t_c} dt\ \tilde{\mathcal{H}}'_{IS}(t) \tag{14}$$

$$\bar{\mathcal{H}}_{IS}^{(1)} = \frac{-i}{2\ t_c} \int_0^{t_c} dt \int_0^{t} dt'\ [\tilde{\mathcal{H}}'_{IS}(t), \tilde{\mathcal{H}}'_{IS}(t')] \tag{15}$$

$$\bar{\mathcal{H}}_{IS}^{(2)} = \frac{-i}{6\ t_c} \int_0^{t_c} dt \int_0^{t} dt' \int_0^{t'} dt''\ \{[\tilde{\mathcal{H}}'_{IS}(t), [\tilde{\mathcal{H}}'_{IS}(t'), \tilde{\mathcal{H}}'_{IS}(t'')]] + [\tilde{\mathcal{H}}'_{IS}(t'')[\tilde{\mathcal{H}}'_{IS}(t'), \tilde{\mathcal{H}}'_{IS}(t)]]\} \tag{16}$$

and we neglect higher order terms. t_c and $\tilde{\mathcal{H}}'_{IS}(t)$ are defined by:

$$t_c = \frac{2\pi}{\omega_e} \tag{17}$$

and:

$$\tilde{\mathcal{H}}'_{IS}(t) = e^{it\omega_e I_z}\ \mathcal{H}'_{IS}\ e^{-it\omega_e I_z} \tag{18}$$

We find by explicit evaluation, inserting (18) and (10) into (14)-(16):

$$\bar{\mathcal{H}}_{IS}^{(0)} = \cos\theta\ S_z \sum_j b_j I_{jz} \tag{19}$$

$$\bar{\mathcal{H}}_{IS}^{(1)} = \sin\theta\ \frac{1}{\omega_e}\ S_z^2 \sum_j b_j^2\ (\cos\theta\ I_{jx} - \tfrac{1}{2}\sin\theta\ I_{jz}) \tag{20}$$

$$\bar{\mathcal{H}}_{IS}^{(2)} = \sin\theta\ \frac{1}{\omega_e^2}\ S_z^3 \sum_j b_j^3\ (P_2(\cos\theta) I_{jx} - \sin\theta\ \cos\theta\ I_{jz}) \tag{21}$$

The expressions (19)-(21) summarize the desired result, namely the leading terms in the interaction between I and S spins. We have gone to $\bar{\mathcal{H}}_{IS}^{(2)}$ and not stopped at $\bar{\mathcal{H}}_{IS}^{(1)}$ since we find easily that:

$$[\bar{\mathcal{H}}_{IS}^{(1)}, S_x] = 0 \tag{22}$$

and thus $\bar{\mathcal{H}}_{IS}^{(1)}$ does not directly affect the S spectrum. Thus in the case that $\bar{\mathcal{H}}_{IS}^{(0)} = 0$ we must go to the next contributing term $\bar{\mathcal{H}}_{IS}^{(2)}$. Decoupling will be efficient when $\bar{\mathcal{H}}_{IS}^{(0)}$ and $\bar{\mathcal{H}}_{IS}^{(2)}$ become small. From (19) this means first of all

$$\cos\theta \sim 0 \tag{23}$$

i.e., from (12) the onset of decoupling occurs when ω_1 starts to get larger than $\Delta\omega$.

$$\omega_1 \gtrsim \Delta\omega \tag{24}$$

From (21) this means secondly, using (23) and (11) i.e., taking $\theta = 90°$:

$$\omega_1 \gtrsim D \tag{25}$$

where D roughly characterizes the strength of the dipolar coupling and can be written as the square root of the second moment of the line due to the operator part of (21) with $\theta = 90°$

$$D^3 = \frac{1}{2}\left(\frac{\mathrm{Tr}[S_z^3 \sum_j I_j^3 I_{jx}, S_x]^2}{\mathrm{Tr}\, S_x^2}\right)^{1/2} \tag{26}$$

Equations (24) and (25) express what we expect, that ω_1 must cover both the resonance offset $\Delta\omega$ and the dipolar broadening, (namely the larger of the two) for the onset of spin decoupling.

C. Asymptotic Behavior of S Linewidth

The asymptotic functional dependence of the S linewidth for large ω_1 on $\Delta\omega$ and ω_1 can also be extracted and we do so for two experimental situations.

1. Off resonance decoupling

Assume the rigid S half linewidth at half height with no I irradiation is given by δ_o, and the S half linewidth at half height with decoupling is given by δ. We investigate how δ/δ_o depends on $\Delta\omega$ for large ω_1. Since ω_1 is large and we take $\Delta\omega \neq 0$, the leading term in $\bar{\mathcal{H}}'_{IS}$ is given by (19). Thus we see immediately

$$\frac{\delta}{\delta_o} = \cos\theta \tag{27}$$

and from (12) this means:

$$\frac{\delta}{\delta_o} = \frac{\Delta\omega}{\sqrt{\omega_1^2 + \Delta\omega^2}} \tag{28}$$

Thus for small $\Delta\omega$ the asymptotic large ω_1 dependence of $\frac{\delta}{\delta_o}$ on $\Delta\omega$ is given by

$$\frac{\delta}{\delta_o} \sim \frac{\Delta\omega}{\omega_1} \quad , \quad \Delta\omega \neq 0 \quad , \quad \omega_1 \text{ large} \tag{29}$$

2. On resonance decoupling

In this case we assume $\Delta\omega = 0$ and investigate the asymptotic behavior of $\frac{\delta}{\delta_o}$ as a function of ω_1 for large ω_1. The leading term in the S linewidth is assumed to arise from $\bar{\mathcal{H}}_{IS}^{(2)}$ given by (21) since $\bar{\mathcal{H}}_{IS}^{(0)} = 0$ and from (22) $\bar{\mathcal{H}}_{IS}^{(1)}$ can only contribute in higher order via cross terms. We assume in this case the S linewidth to be proportional to the square root of its second moment, which is reasonable for a Gaussian-like lineshape:

$$\frac{\delta}{\delta_o} = \left(\frac{\mathrm{Tr}[\bar{\mathcal{H}}_{IS}^{(2)}, S_x]^2}{\mathrm{Tr}[\mathcal{H}_{IS}, S_x]^2} \right)^{\frac{1}{2}} \tag{30}$$

Which can be calculated from (21) for the case that $\theta = 90°$:

$$\frac{\delta}{\delta_o} = \frac{1}{8\omega_1^2} \left(\frac{\sum_j b_j^6}{\sum_j b_j^2} \right)^{\frac{1}{2}} \tag{31}$$

Assuming a Gaussian like shape for the S line we take for the rigid half linewidth:[2c]

$$\delta_o = 1.18\, M_2^{\frac{1}{2}} \tag{32}$$

where M_2 is the rigid second moment given by:

$$M_2 = \frac{1}{3} I(I+1) \sum_j b_j^2 \tag{33}$$

Using (31)-(33) and defining a dimensionless parameter μ which depends on the lattice:

$$\mu = \frac{\sum_j b_j^6}{(\sum b_j^2)^3} \tag{34}$$

we find finally for the asymptotic behavior of $\frac{\delta}{\delta_o}$

$$\frac{\delta}{\delta_o} = C\mu^{\frac{1}{2}}\left(\frac{\delta_o^2}{\omega_1^2}\right) \qquad \Delta\omega = 0 \quad , \quad \omega_1 \text{ large} \tag{35}$$

where C is a numerical constant easily evaluated from (31)-(34). Note that δ_o is related to the parameter D in (26) and for our assumption of a Gaussian line:

$$D \sim \delta_o \tag{36}$$

So that the rigid linewidth δ_o can be used as the parameter for the decoupling criterion, i.e.,

$$\omega_1 \gtrsim \Delta\omega \, , \, \delta_o \tag{37}$$

We note here that physically, the decoupling occurs because the applied perturbation $\omega_1 I_x$ is vectorially orthogonal to the coupling operator I_z and causes it to rotate and average to zero. We now apply these considerations to the case of double quantum effects for spin I = 1 where we hope that we can find similar orthogonal vector operators.

III. DOUBLE QUANTUM EFFECTS

In this section we treat the theoretical problem of central interest in this paper, namely that of spins I = 1 coupled to our S spin. This is depicted schematically in Figure 7. The Hamiltonian in the rotating frame is the same as that of equation (6) with the addition of the I spin quadrupolar interaction:

$$\mathcal{H} = -\Delta\omega I_z - \omega_1 I_x + \frac{1}{3}\omega_Q (3I_z^2 - I(I+1)) + \mathcal{H}_{IS} \tag{38}$$

we assume that:

$$\Delta\omega, \omega_1 \ll \omega_Q \tag{39}$$

i.e., we irradiate near the center of the quadrupolar spectrum with an ω_1 much smaller than ω_Q.

We next show that in the limit $\frac{\omega_1}{\omega_Q} \ll 1$ the problem of decoupling $\mathcal{H}_{IS}$ reduces to a spin-½ problem.

A. Fictitious Spin-½ Operators

Following the theory of double quantum nmr[6] we define the following nine fictitious spin-½ operators[7] $I_{p,i}$ in terms of the spin-1 angular momentum operators I_p:

$$\begin{aligned} I_{p,1} &= \frac{1}{2} I_p \\ I_{p,2} &= \frac{1}{2} (I_q I_r + I_r I_q) \\ I_{p,3} &= -\frac{1}{2} (I_q^2 - I_r^2) \end{aligned} \qquad \begin{aligned} &p,q,r = x,y,z \text{ or} \\ &\text{cyclic permutation} \end{aligned} \tag{40}$$

The usefulness of these operators derives from the fact that for each p(p = x,y,z) the $I_{p,i}$ fulfill spin-½ angular momentum commutation relations:

$$[I_{p,i}, I_{p,j}] = iI_{p,K} \qquad \begin{matrix} i,j,k = 1,2,3 \text{ or} \\ \text{cyclic permutation} \end{matrix} \qquad (41)$$

Thus each p describes a fictitious two level spin-½ subspace with three orthogonal vector operators. Each is an SU(2) subgroup of the full SU(3) group. We term the subspace corresponding to p the p- space. In particular, the $I_{z,i}$ operators have matrix elements only between the I = 1 levels m = ±1 and thus correspond to double quantum transitions. They are termed double quantum operators and the z- space is often called the double quantum frame.[7] In many cases, the frames are uncoupled from each other, i.e., the evolution of the operators does not involve changes in p, only independent rotations in each p- space. We shall see shortly that such is the case for double quantum irradiation and we shall thus have found the orthogonal operators required for double quantum spin decoupling.

Note that we can equally well use the fictitious spin-½ operators in the I_z basis described by Vega and by Ernst, et al.[6] in all that follows by making the correspondence

$$-I_{z,3} \rightarrow I_x^{1-3}$$

$$I_{z,2} \rightarrow I_y^{1-3}$$

$$I_{z,1} \rightarrow I_z^{1-3}$$

where I_p^{i-j} means a σp Pauli spin operator between levels i and j.

Rewriting the Hamiltonian (38) in terms of the spin-½ operators (40) we have:

$$\mathcal{H} = -2\Delta\omega I_{z,1} - 2\omega_1 I_{x,1} + \frac{2}{3}\omega_Q(I_{x,3}-I_{y,3}) + \mathcal{H}_{IS} \tag{42}$$

where:

$$\mathcal{H}_{IS} = 2 S_z \sum_j b_j I_{jz,1} \tag{43}$$

We now apply a transformation to a tilted frame with the operator:

$$T_{x,2} = e^{i\psi_x I_{x,2}} \tag{44}$$

where:

$$\psi_x = \tan^{-1}\frac{2\omega_1}{\omega_Q} \tag{45}$$

Remembering that $\omega_1 << \omega_Q$ from (30), i.e., $\psi_x \sim 0$, the transformed Hamiltonian in this new frame can be written to a good approximation as:[6]

$$\mathcal{H} \simeq -2\Delta\omega I_{z,1} - \frac{\omega_1^2}{\omega_Q} I_{z,3} + \frac{2}{3}\omega_Q(I_{x,3}-I_{y,3}) + \mathcal{H}_{IS} \tag{46}$$

The third term $\frac{2}{3}\omega_Q(I_{x,3}-I_{y,3})$ commutes with all the other terms in the Hamiltonian and can be dropped since it will have no effect on the decoupling. We thus obtain finally:

$$\mathcal{H}_{DQ} \simeq -2\Delta\omega I_{z,1} - \frac{\omega_1^2}{\omega_Q} I_{z,3} + \mathcal{H}_{IS} \tag{47}$$

with $\mathcal{H}_{IS}$ given by (43). The subscript DQ is placed to denote double quantum, since only $I_{z,i}$ (or I_p^{1-3} in the alternative notation) operators appear in the effective Hamiltonian. The operator $\frac{\omega_1^2}{\omega_Q} I_{z,3}$ is an effective rf field operator which induces transitions between m = ±1 and was used to explain our Fourier transform double quantum nmr experiments and double quantum spin locking.[8] (Figure 8) depicts the double quantum transition schematically.

Equation (47) is now formally identical to equation (6) for the spin-½ case . We identify I_z, and I_x in the latter case with our $I_{z,1}$ and $I_{z,3}$ double quantum operators respectively, and $\Delta\omega$ and ω_1 with $2\Delta\omega$ and $\frac{\omega_1^2}{\omega_Q}$ respectively. $\mathcal{H}_{IS}$ also has the same form with I_{jz} replaced by $2I_{jz,1}$ according to (40). Thus the system behaves like a fictitious spin-½ case in double quantum space with effective resonance offset field $2\Delta\omega$ along the z,1 axis and effective rf field $\frac{\omega_1^2}{\omega_Q}$ along the z,3 field. Figure 9 summarizes this section by depicting the double quantum frame Hamiltonian schematically.

B. Double Quantum Decoupling

The Hamiltonian in equation (47) contains three terms; a resonance offset $2\Delta\omega$ an effective rf field $\frac{\omega_1^2}{\omega_Q}$ and the I-S coupling. We now wish to calculate the effect of the first two terms in (47) on the third, $\mathcal{H}_{IS}$, which is reponsible for the broadening of the S line. Equation (41) ensures that the operator $I_{z,1}$ will precess about the effective field defined by the first two terms in (47) depicted in Figure 9. This will cause a coherent averaging of $\mathcal{H}_{IS}$. We have solved exactly this problem in Section IIB, and we proceed by analogy here by first

transferring to a tilted frame defined so that the effective field is along the z,1 axis in the double quantum frame: The transformation operator is by direct analogy to (8):

$$T_{z,2} = \exp(-i\ \theta_D\ I_{z,2}) \tag{48}$$

where:

$$\theta_D = \tan^{-1} \frac{\omega_1^2}{2\Delta\omega\ \omega_Q} \tag{49}$$

and from (47) the transformed Hamiltonian is given by direct analogy with (9):

$$\mathcal{H}'_{DQ} = -\omega_e I_{z,1} + \mathcal{H}'_{IS} \tag{50}$$

where

$$\omega_e = ((2\Delta\omega)^2 + \frac{\omega_1^4}{\omega_Q^2})^{\frac{1}{2}} \tag{51}$$

again the subscript D on θ_D and ω_{eD} serve to indicate that this is the double quantum case, distinguished from the θ and ω_e in the spin-$\frac{1}{2}$ case.

Now applying coherent averaging theory assuming $\omega_e >> ||\mathcal{H}_{IS}||$ we obtain by analogy with (19) and (21) using (43) for $\mathcal{H}_{IS}$:

$$\bar{\mathcal{H}}^{(0)}_{IS} = 2\cos\theta_D\ S_z \sum_j b_j I_{jz,1} \tag{52}$$

$$\bar{\mathcal{H}}^{(1)}_{IS} = 4\sin\theta_D \frac{1}{\omega_{eD}} S_z^2 \sum_j b_j^2\ (\cos\theta_D\ I_{jz,3} - \frac{1}{2}\sin\theta_D\ I_{jz,1}) \tag{53}$$

$$\bar{\mathcal{H}}_{IS}^{(2)} = 8\sin\theta_D \frac{1}{\omega_e{}^2{}_D} S_z{}^3 \sum_j b_j{}^3 \left(P_2(\cos\theta_D) I_{jz,3} - \sin\theta_D \cos\theta_D I_{jz,1}\right) \tag{54}$$

The decoupling conditions for the double quantum case can now be written down easily. We need to make $\bar{\mathcal{H}}_{IS}^{(0)}$ and $\bar{\mathcal{H}}_{IS}^{(2)}$ small, so we demand, from (52):

$$\cos\theta_D \sim 0 \tag{55}$$

and from (54), together with (49), (51) and (55):

$$\frac{\omega_1{}^2}{\omega_Q} \gtrsim D \tag{56}$$

Thus we arrive at the condition for double quantum decoupling stated previously in equation (2) and derived loosely in reference 4.

We now follow Section IIC and derive the quantitative behavior of the S linewidth for large $\frac{\omega_1{}^2}{D\omega_Q}$ on the I spins in the double quantum case.

1. Off resonance double quantum decoupling.

We assume a large $\frac{\omega_1{}^2}{\omega_Q}$ off resonance in analogy to IIC.1. In this case, the residual I-S coupling is dominated by $\bar{\mathcal{H}}_{IS}^{(0)}$ in (52) yielding for the linewidth δ relative to the full undecoupled linewidth δ_o of the S spins:

$$\frac{\delta}{\delta_o} = \cos\theta_D = \frac{2\Delta\omega}{\left((2\Delta\omega)^2 + \frac{\omega_1{}^4}{\omega_Q{}^2}\right)^{\frac{1}{2}}} \tag{57}$$

For large ω_1 such that $\omega_1^2 >> 2\Delta\omega\ \omega_Q$ the asymptotic behavior is:

$$\frac{\delta}{\delta_o} \sim \frac{2\Delta\omega\ \omega_Q}{\omega_1^2} \qquad \Delta\omega \neq 0 \ , \ \omega_1 \text{ large} \tag{58}$$

Note the extreme predicted sensitivity of the double quantum decoupling to the resonance condition, due to the large ω_Q multiplying $\Delta\omega$, in contrast to the normal single quantum decoupling case, equations (28), (29). This sensitivity to resonance was observed by Meiboom et al.[3] in liquid crystal deuterium decoupling, and is borne out by our experiments on solids described in Section IV.

2. On resonance double quantum decoupling

We now have $\Delta\omega = 0$, so $\bar{\mathcal{H}}_{IS}^{(0)} = 0$ and since $\mathcal{H}_{IS}^{(1)}$ is ineffective we calculate $\frac{\delta}{\delta_o}$ using the residual term $\bar{\mathcal{H}}_{IS}^{(2)}$ with $\theta_D = 90°$. Again, assuming for simplicity that the S linewidth is proportional to the square root of its second moment, we can use equation (30) which gives in this case:

$$\frac{\delta}{\delta_o} = \frac{\omega_Q^2}{2\omega_1^4} \left(\frac{\sum_j b_j^6}{\sum b_j^2} \right)^{1/2} \tag{59}$$

We have used the fact that for $\Delta\omega = 0$

$$\omega_{eD} = \frac{\omega_1^2}{\omega_Q} \tag{60}$$

from equation (51). Assuming a Gaussian lineshape we obtain in analogy to equations (32) to (35):

$$\frac{\delta}{\delta_o} = C_D \mu^{\frac{1}{2}} \frac{\delta_o^2 \omega_Q^2}{\omega_1^4} \tag{61}$$

where C_D is a numerical constant and μ is given by (34). C_D is easily evaluated from (32), (33) and (59). δ_o is the rigid S line half width at half height with no I spin decoupling. We therefore predict a more drastic dependence of $\frac{\delta}{\delta_o}$ on ω_1

$$\frac{\delta}{\delta_o} \sim \frac{1}{\omega_1^4} \tag{62}$$

than in the single quantum case which depends on $\frac{1}{\omega_1^2}$ as in equation (35).

A summary of the decoupling conditions appears in Figure 10 showing the relaxed ω_1 requirement for double quantum decoupling.

IV. EXPERIMENTS

A. Experimental Details

Experiments were done on samples of deuterated dimethylsulfoxide (DMSO-d_6) deuterated benzene (C_6D_6) and heavy water (D_{20}). In all cases the samples were deuterated to > 99% and the residual < 1% protons were observed while decoupling the deuterium under different conditions. Since all these materials are liquids at room temperature, they were cooled by gaseous nitrogen for the solid state work. The most appealing way to do the experiments would be to use single crystals with well defined ω_Q values. However, as seen in Figures 3 and 4 even in a powder most of the deuterium spectral intensity is concentrated in a small region of ω_Q values near the singularities. This is especially so in the present case where the electric field gradient tensors are close to axially symmetric. Thus we take these to be the effective ω_Q values in all our samples. For DMSO 2 ω_Q = 44 kHz and for benzene 2 ω_Q = 70 kHz, giving us two independent values on which to check our theory.

The spectrometer used in these experiments was similar to that described previously for our ^{13}C work[9], modified for deuterium-proton double resonance. The deuterium decoupling amplifier was a modified radio amateur transmitter producing several hundred watts of rf power at 16.3 MHz. A schematic diagram of the spectrometer and the homebuilt probe are shown in Figure 11. Calibration of the rf fields ω_1 was performed both by normal single quantum experiments on the liquid samples and by double quantum rotary decays on the solid samples.[8]

B. Deuterium Decoupled Spectra

As a qualitative introduction to the type of spectra observed experimentally with deuterium decoupling we show some simple illustrative examples. Figure 12 shows three spectra indicating the effect of double quantum decoupling on the residual protons in a perdeuterated ($\sim$ 99.5% deuterium) sample of DMSO. In the solid the deuterium quadrupolar broadening is large as indicated in Figure 4. The effect of a moderate rf field on the deuterium with $\omega_1 << \omega_Q$ is sufficient to effect spin decoupling. As expected for the double quantum process, this is very sensitive to deuterium frequency and is discussed in more detail in the next section. Also shown is an isotropic liquid spectrum of the same sample for comparison.

The onset of double quantum decoupling is shown in more detail in Figure 13. At an rf intensity of ν_1 = 10.4 kHz the residual ^1H spectrum is completely decoupled and a further increase in rf intensity to ν_1 = 46.5 kHz serves only to induce an appreciable Bloch-Siegert shift.[10] The ^1H linewidth under decoupling conditions is determined by a combination of ^1H-^1H dipolar coupling and by anisotropy of the bulk magnetic susceptibility.[4]

One of the potential applications of double quantum deuterium decoupling is the resolution of ^1H-^1H dipolar couplings in selectively doped proton groups in a deuterated host. For example, the study of quantum mechanical tunneling in methyl groups at low temperatures would benefit from this.[12] Figure 14 indicates that indeed fine structure is apparent in the residual ^1H spectrum when 10% protonated

DMSO is doped into a deuterated host. The additional peaks arise from intramolecular and intermolecular dipolar couplings.

As a final example of the resolution obtained by double quantum decoupling we depict in Figure 15 the residual ^1H spectra obtained in deuterated ice and presented in our preliminary communication.[4] This constitutes the first measurement of the proton chemical shift anisotropy in ice, a material in which there is a great deal of interest and for which many other measurements and calculations have been made.[13] Of particular interest are the atomic and molecular motions in ice, which are responsible for various relaxation mechanisms. By studying the ^1H lineshape as a function of temperature, we have been able to separate out and characterize clearly for the first time that component of the relaxation arising from proton motion amongst sites related by tetrahedral symmetry.[14] The value of $\Delta\sigma = 34 \pm 4$ ppm for the chemical shift is similar to that obtained recently using a multiple pulse technique.[15]

C. Dependence on rf Intensity and Resonance Offset

In this section we present experimental results designed to investigate the sensitivity of the double quantum decoupling to the I resonance condition (equation (48)) and the $\frac{1}{\omega_1^4}$ dependence on rf intensity (equation (52)). Firstly, the resonance offset behavior was investigated on perdeuterated dimethylsulfoxide at -75°C. The extra linewidth of the residual protons due to ^2D coupling was observed as the ^2D spins were irradiated with a constant rf field (ν_1) at several frequencies. The dependence of the excess proton linewidth

as function of the offset from deuterium resonance for four values of ν_1 is shown in Figure 16. The calculated solid curves are from equation (57) with no adjustable parameters. Similar behavior is observed in a completely different sample, perdeuterated benzene at -35°C as shown in Figure 17 for a ν_1 of $\sim$ 10 kHz. Note in both cases the good agreement between theory and experiment with no adjustable parameters, and the sensitivity of the decoupling to the deuterium resonance condition.

The dependence of the decoupling on rf field intensity ν_1 was checked on the same two samples. In Figure 18 the dependence of residual proton linewidth is shown as a function of deuterium ν_1 applied at resonance in DMSO-d_6. The solid line is the asymptotic $\frac{1}{\nu_1^4}$ dependence from equation (61). The dashed line indicates the behavior we would expect if the decoupling had to proceed through the allowed single quantum transitions. Figure 19 shows analogous results for benzene-d_6. In both cases we get excellent agreement between experiment and the behavior predicted for pure double quantum effects both for the onset of decoupling and for the asymptotic $\frac{1}{\nu_1^4}$ behavior.

D. Lineshapes and Linewidths

In the previous sections we were interested in the S-linewidth dependence on $\Delta\nu$ and ν_1 (for large ν_1) of the I-spin. It is possible to be somewhat more precise and we make here some brief comments about the S lineshape and about the ν_1 dependence for finite ν_1. The S lineshape is given by the Fourier transform of the free induction decay function:[16]

$$G(t) = \mathrm{Tr}\{e^{-i\mathcal{H}t} S_x e^{i\mathcal{H}t} S_x\}/\mathrm{Tr}\, S_x^2 \qquad (63)$$

where $\mathcal{H}$ is the spin Hamiltonian. In the case that I is a spin-½ the appropriate $\mathcal{H}$ in the rotating frame is given by equation (6). If we do not decouple, i.e., $\omega_1 = 0$, then the trace in (63) can be evaluated explicitly, yielding:

$$G(t) = \prod_j \cos(\tfrac{1}{2} b_j t) \qquad I = \tfrac{1}{2},\ \omega_1 = 0 \tag{64}$$

If the I spins are irradiated off resonance by $\Delta\omega$ with a large ω_1 then the appropriate Hamiltonian is that in equation (19) and again the trace can be evaluated explicitly by replacing b_j in (64) with $\cos\theta\ b_j$ where θ is given by (12):

$$G(t) = \prod_j \cos(\tfrac{1}{2} b_j t) \qquad I = \tfrac{1}{2},\ \text{large } \omega_1 \tag{65}$$

Thus, we see that in the case of single quantum decoupling the S-lineshape does not change as the large I ω_1 is shifted off resonance and only scales in width as $\cos\theta$.

What happens in the case of I being spin-1 and subject to double quantum decoupling? The appropriate Hamiltonian is given in equations (42) and (43). Again, for no irradiation on I the trace in (63) is explicitly evaluated as:

$$G(t) = \prod_j \tfrac{1}{3} (1 + 2 \cos b_j t) \qquad I = 1,\ \omega_1 = 0 \tag{66}$$

If the I spins are now irradiated at $\Delta\omega$ from resonance with a large $\frac{\omega_1^2}{\omega_Q}$, then the appropriate Hamiltonian is given by equation (52) and thus evaluation of the trace in (63) is the same as (66)

with replacement of b_j by $\cos\theta_D\, b_j$ where θ_D is defined in (49):

$$G(t) = \prod_j \frac{1}{3}\left(1 + 2\cos\left(\cos\theta_D\, b_j t\right)\right) \tag{67}$$

We have not verified this double quantum lineshape and scaling effect quantitatively, but it certainly would be interesting to do so.

Finally, in this section we discuss the dependence of the S linewidth on the I = 1 irradiation strength ω_1 at resonance. The asymptotic behavior for large $\frac{\omega_1^2}{\omega_Q}$ was described in equations (59)-(61) and experimental results were shown in Figures 18 and 19. The question is whether we can say something about the lineshape under these conditions and also about the ω_1 dependence over the whole ω_1 range. At resonance, the appropriate Hamiltonian in (63) for double quantum decoupling with large $\frac{\omega_1^2}{\omega_Q}$ is given by (54) with $\theta_D = 90°$. The trace can be evaluated and yields the same as (66) if b_j is replaced by:

$$\bar{b}_j = \lambda_j b_j \qquad \text{large } \frac{\omega_1^2}{\omega_Q} \tag{68}$$

where:

$$\lambda_j = \frac{b_j^2\, \omega_Q^2}{2\,\omega_1^4} \tag{69}$$

Thus, for large $\frac{\omega_1^2}{\omega_Q}$ the S-lineshape should still remain the same and be scaled by (69). To account for the full (including small ω_1 and no decoupling) ω_1 dependence, we assume

$$\bar{b}_j = \frac{\lambda_j}{1 + \lambda_j} \tag{70}$$

This reduces to the correct limits for $\omega_1 \to 0$ (no decoupling) and $\omega_1 \to \infty$ (asymptotic behavior) and is found to be an excellent assumption in exact calculation on a small number of spins. Using (70), the dependence of S-linewidth on I-ω_1 at resonance can be explicitly calculated; assuming that the linewidths are proportional to the second moments as in equation (32) we find:

$$\frac{\delta}{\delta_o} = [1 + (\frac{\omega_1}{\omega_1^*})^4]^{-1} \tag{71}$$

where ω_1^* can obviously be regarded as a threshold decoupling intensity and is given by

$$\omega_1^{*4} = (1.18)^2 \frac{2}{3} I(I + 1) \mu^{\frac{1}{2}} \omega_Q^2 \delta_o^2 \tag{72}$$

Equation (71) thus provides an extension of (61) to the full ω_1 range.

Figure 20 demonstrates that indeed (72) predicts the ω_1 dependence on resonance of the S linewidth quite well. The experimental data from Figure 18 are compared this time with the full expression in (71) yielding a best value for the threshold decoupling intensity of

$$\frac{\omega_1^*}{2\pi} = 7.4 \text{ KHz}$$

which agrees quite well with the value estimated from the lattice constants for DMSO.

V. COUPLED SPINS AND MULTIPLE QUANTUM EFFECTS

In this section we mention two rather natural extensions of the double quantum effects described in this paper, namely to an I spin system which consists itself of coupled spins-½ (e.g., 2 strongly coupled protons (I) coupled to $^{13}C(s)$) and secondly to higher order multiple quantum effects (e.g., I > 1 or several coupled spins-½). These extensions are obvious not only to the spin decoupling phenomena, but also to multiple quantum coherence, i.e., the excitation and detection of specific multiple quantum transitions for spin I > 1 or for coupled spin-½ systems. This latter extension to Fourier transform multiple quantum spectroscopy will be described in detail elsewhere.

As a simple example of a coupled spin-½ system we take 2 equivalent protons (I) coupled equally to another spin-½ (S) as described in Figure 21. This is a system of practical interest, since $^{1}H_2$-^{13}C groups occur in the aliphatic chains of liquid crystals, polymers and biological membranes where NMR studies are of great importance. We wish to know the two I spins are decoupled from the S-spin by irradiating them near resonance. The Hamiltonian is given by:

$$\mathcal{H} = \mathcal{H}_{II} + \mathcal{H}_{IS} \tag{73}$$

where in the rotating frame at resonance for S and off resonance by $\Delta\omega$ for I:

$$\mathcal{H}_{II} = -\Delta\omega(I_{1z} + I_{2z}) + \frac{2}{3} a\ (3I_{1z}I_{2z} - \underset{\sim}{I}_1 \cdot \underset{\sim}{I}_2)$$

$$-\omega_1(I_{1x} + I_{2x}) \tag{74}$$

$$\mathcal{H}_{IS} = b(I_{1z} + I_{2z})S_z \tag{75}$$

We know that two equivalent coupled protons produce orthogonal singlet and triplet states.[17] We expect that the singlet does not couple to the S spin and that the triplet can be treated identically to the spin I = 1 problem in the previous sections. We thus define double quantum fictitious spin-½ operators I_p^{i-j} [6(b)] for the $|-\frac{1}{2},-\frac{1}{2}\rangle$ (denote this state $|-1\rangle$ by i = 1) to $|\frac{1}{2},\frac{1}{2}\rangle$ (denote this state $|+1\rangle$ by j = 4) proton transitions:

$$\begin{aligned} I_x^{1-4} &= (I_{1x}I_{2x} - I_{1y}I_{2y}) \\ I_y^{1-4} &= (I_{1x}I_{2y} + I_{1y}I_{2x}) \\ I_z^{1-4} &= \tfrac{1}{2}\,(I_{1z} + I_{2z}) \end{aligned} \tag{76}$$

These behave exactly as $-I_{z,3}$, $I_{z,2}$ and $I_{z,1}$ of Section III. They are a special case of the general fictitious spin-½ operators I_p^{i-j} defined by Vega and by Ernst, et al.,[6(b)] in a multilevel system. Levels 2 and 3 refer to the singlet and the remaining triplet state which do not enter the DQ behavior.

Proceeding now by exact analogy to the double quantum condition of Section III, in the case that $\omega_1 \ll a$, we transform the Hamiltonian in (73) by the infinitessimal transformation operator analogous to (44) with the angle

$$\psi = \tan^{-1}\ \frac{2\omega_1}{a} \tag{77}$$

yielding to a good approximation the effective double quantum Hamiltonian:

$$\mathcal{H}_{DQ} \simeq -2\Delta\omega\ I_z^{1-4} + \frac{\omega_1^2}{a}\ I_x^{1-4} + 2bI_z^{1-4}\ S_z \tag{78}$$

The term proportional to $(3I_{1z}I_{2z} - \underset{\sim}{I}_1 \cdot \underset{\sim}{I}_2)$ commutes with $\mathcal{H}_{DQ}$ and with I_z^{1-4} and has thus been dropped since it will not affect the experiment. The problem is now formally identical to the spin-1 case (equation (47)) and the decoupling conditions at resonance can be written down immediately:

$$\frac{\omega_1^2}{a} \gtrsim b \tag{79}$$

Thus, the rf intensity does not always need to be larger than the I spectral width (a) as is commonly thought. The two I spins can be made to flip coherently up and down by the resonant double quantum process more easily than each one separately. This effect was noticed previously in our liquid crystal work where moderate ω_1 fields on protons decoupled them from ^{13}C spins on aliphatic end chains despite the strong proton-proton couplings.[4,18] All the other analogous properties to spin-1 may be treated in a similar fashion.

As a final simple example consider the case of a spin $I = \frac{3}{2}$ (relevant to lithium NMR) coupled to spin $S = \frac{1}{2}$ in high magnetic ield. In direct extension of the double quantum ideas, Figure 22 shows that here we expect resonant triple as well as single quantum transitions.[6(b)] The cross section in the regime $\omega_1 << \omega_Q$ for the triple quantum transitions

should go as $\frac{\omega_1^3}{\omega_Q^2}$ from 3rd order perturbation theory;[4] more precisely it is given by $\frac{3\omega_1^3}{2\omega_Q^2}$ where $2\omega_Q$ is the full width of the I spectrum. Thus, as shown in Figure 23 we expect that when a resonant rf field of intensity ω_1 is applied to the $I = \frac{3}{2}$ spins the $\pm \frac{3}{2}$ transition should flip at a rate of $\frac{3\omega_1^3}{2\omega_Q^2}$ and the $\pm \frac{1}{2}$ single quantum transition at $2\omega_1$. Thus the condition for the onset of decoupling in this case and observation of a sharp S signal is:

$$\omega_1^3 \gtrsim D\omega_Q^2 \tag{80}$$

where again D characterizes the I-S dipolar coupling (a particular coupling b is shown in Figure 23). The extension to spin $\frac{N}{2}$:

$$\omega_1^N \gtrsim D\omega_Q^{N-1} \tag{81}$$

is straightforward.

Similar considerations can be applied to N equivalent coupled protons. As mentioned previously[4] under contions where the proton-proton coupling is much stronger than the proton S-spin coupling, the proton system behaves in many respects as an independent set of spins N+1, N-1, ... which should exhibit multiple quantum effects of the type discussed above. Note that as N gets large the criterion (81) approaches the accepted rule that ω_1 must be of the order of the stronger I-I coupling.

Acknowledgment

This work was supported by the Energy Research and Development Association, Division of Physical Research. Partial support by NATO is also gratefully acknowledged. We thank Dr. D. J. Ruben and D. E. Wemmer for helpful conversations and for their assistance with experimental problems.

References and Footnotes

† Permanent address: Department of Isotope Research, Weizmann Institute of Science, Rehovot, Israel.

‡ Permanent address: Institute of Physics, University of Dortmund, Dortmund, West Germany.

1. F. Bloch, Phys. Rev. 111, 841 (1958); L. R. Sarles and R. M. Cotts, Phys. Rev. 111, 853 (1958).
2. A. Pines, M. G. Gibby and J. S. Waugh, J. Chem. Phys., 59, 569 (1973); M. Mehring and G. Sinning, Phys. Rev. B 15, 2519 (1977).
3. R. C. Hewitt, S. Meiboom and L. C. Snyder, J. Chem. Phys., 58, 5089 (1973); L. C. Snyder and S. Meiboom, J. Chem. Phys., 58, 5096 (1973).
4. A. Pines, D. J. Ruben, S. Vega and M. Mehring, Phys. Rev. Lett., 36, 110 (1976).
5. U. Haeberlen and J. S. Waugh, Phys. Rev., 185, 420 (1969), U. Haeberlen, in "Advances in Magnetic Resonance", 1976 Supplement, Academic, N.Y. (1976); M. Mehring, "High Resolution NMR Spectroscopy", Springer Verlag, Berlin (1976).
6. (a) S. Vega, T. W. Shattuck and A. Pines, Phys. Rev. Lett., 37, 43 (1976); S. Vega and A. Pines, J. Chem. Phys., 66, 5624 (1977);
   (b) S. Vega, J. Chem. Phys., in press, R. R. Ernst, private communication; A. Wokaun and R. R. Ernst, J. Chem. Phys., in press.
7. A. Abragam, "The Principles of Nuclear Magnetism", Oxford University Press, (1961); R. P. Feynman, F. L. Vernon and R. W. Hellworth, J. Appl. Phys., 28, 49 (1957); H. Hatanaka, T. Terao and T. Hashi,

J. Phys. Soc. Jap., 39, 835 (1975).

8. A. Pines, et al., Multiple Quantum NMR, International Summer School on Magnetic Resonance and Phase Transitions, Pula, Yugoslavia, September, 1976; S. Vega and A. Pines in "Magnetic Resonance and Related Phenomena", p. 183, 19th Ampere Congress, Heidelberg, Germany, September, 1976; D. G. Gold and E. L. Hahn, Phys. Rev. A, 16, 324 (1977).
9. T. W. Shattuck, Supplement to Ph.D. thesis, Berkeley (1976).
10. F. Bloch and A. Siegert, Phys. Rev., 57, 522 (1970).
11. The dependence of the ^{1}H linewidth on concentration (level of deuteration) has been measured and ^{1}H multiple-pulse experiments together with double quantum decoupling have been performed to check this. Results will be presented separately.
12. C. Mottley, T. B. Cobb and C. S. Johnson, J. Chem. Phys., 55, 5823 (1971).
13. D. E. Barnaal and I. J. Lowe, J. Chem. Phys., 46, 4800 (1967); L. Onsager and L. K. Remnels, J. Chem. Phys., 50, 1089 (1969); H. Granicher, in "Physics of Ice", Plenum N.Y. (1969).
14. D. E. Wemmer, D. J. Ruben and A. Pines, Some preliminary details of this ^{1}H dynamics study in ice appears in the first entry of reference 8.
15. B. Gerstein, private communication.
16. I. J. Lowe and N. E. Norberg, Phys. Rev., 107, 46 (1957).
17. C. P. Slichter, "Principles of Magnetic Resonance", Harper and Row, N.Y. (1963).
18. A. Pines, D. F. Ruben and S. Allison, Phys. Rev. Lett., 33, 1002 (1974).

Figure Captions

1. Schematic description of spin decoupling. We wish to observe spins S whose resonance is broadened by interaction with spins I. Irradiation of the I spins with near resonant radio frequency radiation under the appropriate conditions serves to decouple them from the S spins giving a lengthened free induction decay following the S-pulse.
2. Spin I = 1 in high magnetic field. The degenerate allowed transitions are split by the quadrupolar interaction into two lines separated by $2\omega_Q$. For deuterium the quadrupolar coupling parameter is typically of the order of $\frac{\omega_Q}{2\pi} \sim 100$ kHz. Thus it is difficult to "cover" the allowed I transitions with practical values of ω_1.
3. Expected spectrum for polycrystalline arrangement of deuterium spins with axially symmetric electric field gradient tensor. For deuterium the maximum width of such a spectrum is typically of the order of ~ 100 kHz.
4. Center portion of deuterium Fourier transform NMR spectrum of solid dimethylsulfoxide-d_6 (DMSO-d_6). The total width of the spectrum is 88 kHz.
5. Possible schemes for deuterium spin decoupling.
6. Spin decoupling case when I = ½, S = ½ showing coupled spins, typical spectrum and I energy levels. Applying a resonant rf field of intensity ω_1 to the I spins splits the ± ½ levels in the rotating frame by ω_1, thus causing inversions of the I spins

at a rate ω_1 relative to the S spins. The tilted rotating frame refers to the rotating frame and then to a tilt which diagonalizes the Hamiltonian putting z along ω_1.

7. Spin decoupling case when I = 1, S = ½ showing coupled spins, typical spectrum and I energy levels. Applying a resonant rf field of intensity ω_1 to the I spins such that $\omega_1 << \omega_Q$ splits the ± 1 levels in the rotating frame by ω_1^2/ω_Q thus causing inversions of the I spins at a rate $\frac{\omega_1^2}{\omega_Q}$ relative to the S spins.
8. Schematic description of double quantum transitions at exact Larmor frequency ω_o causing ± 1 inversions with no appreciable effect on 0.
9. Schematic description of effective fields in double quantum frame. The operators $I_{z,1}$, $I_{z,2}$ and $I_{z,3}$ (axes 1,2,3) can be replaced by I_z^{1-3}, I_y^{1-3}, and I_x^{1-3} to conform to the more general definitions and notation of reference 6(b).
10. Summary of spin decoupling conditions for deuterium with large quadrupolar splitting ω_Q coupled weakly (D ∿ b) to spins S.
11. Schematic of spectrometer used for some of the ^2D-^1H experiments.
12. Demonstration of double quantum spin decoupling in solid. The residual protons in perdeuterated DMSO-d_6 are observed, top with no deuterium irradiation. At center is the spectrum when the deuterium spins are irradiated at resonance with a moderate (ν_1 ∿ 10 kHz) rf field. The deuterium spectrum is much wider than 10 kHz as shown in Figure 4.
13. Dependence of residual proton spectrum in solid DMSO-d_6 on intensity $\nu_1 = \frac{\omega_1}{2\pi}$ of deuterium rf irradiation. At ν_1 ∿ 10 kHz

the spins are essentially completely decoupled and a further increase in ω_1 causes only an appreciable Bloch-Siegert shift.

14. Resolution of ^1H-^1H dipolar coupling fine structure in solid DMSO-h_6 doped 10% into a lattice of DMSO-d_6.

15. Resolution of the chemical shift spectrum for residual protons in heavy ice without (top) and with (bottom) deuterium double quantum spin decoupling. The deuterium spectral width in this case is $\sim$ 230 kHz.

16. Behavior of the excess proton linewidth in DMSO-d_6 at -75°C caused by deuterium dipolar coupling as the deuterium spins are irradiated at various frequencies $\Delta\nu$ from resonance. Note the sensitivity of the decoupling condition to the I resonance condition, a characteristic of the double quantum decoupling process. The solid lines are theoretical calculated in the text.

17. Same as Figure 16 for residual protons in solid perdeuterated benzene at -35°C.

18. Behavior of the excess proton linewidth in DMSO-d_6 at -75°C as the deuterium spins are irradiated at resonance with various values of ω_1 to induce double quantum decoupling. The solid line shows the asymptotic $\frac{1}{\omega_1^4}$ behavior expected from theory as explained in the text. The dashed line shows the expected behavior if double quantum transitions did not occur.

19. Same as Figure 18 for residual protons in solid perdeuterated benzene at -35°C.

20. Comparison of the data in Figure 18 with the full theoretical ω_1 dependence of the linewidth calculated from equation (71) with $\frac{\omega_1^*}{2\pi}$ = 7.4 kHz.

21. Spin decoupling case for two equivalent spins I = ½ coupled strongly (a) to each other and weakly (b) to a spin-S, showing coupled spins, typical spectrum and I energy levels. The triplet manifold $|\pm 1\rangle_T$, $|0\rangle_T$ of the I spins behaves exactly as the spin I = 1 case in Figure 7 with ω_Q replaced by a.

22. Schematic description of triple quantum transition in spin I = $\frac{3}{2}$ system with $\omega_1 << \omega_Q$. The splitting is $\omega_A - \omega_C = 2\omega_Q$.

23. Spin decoupling case when I = $\frac{3}{2}$, S = $\frac{1}{2}$, showing coupled spins, typical spectrum and I energy levels. Applying a resonant rf field of intensity ω_1 to the I spins splits the $\pm \frac{1}{2}$ levels in the rotating frame by $2\omega_1$ and the $\pm \frac{3}{2}$ levels by $\frac{3}{2}\frac{\omega_1^2}{\omega_Q}$ thus causing inversions of these pairs of level at the above frequencies.

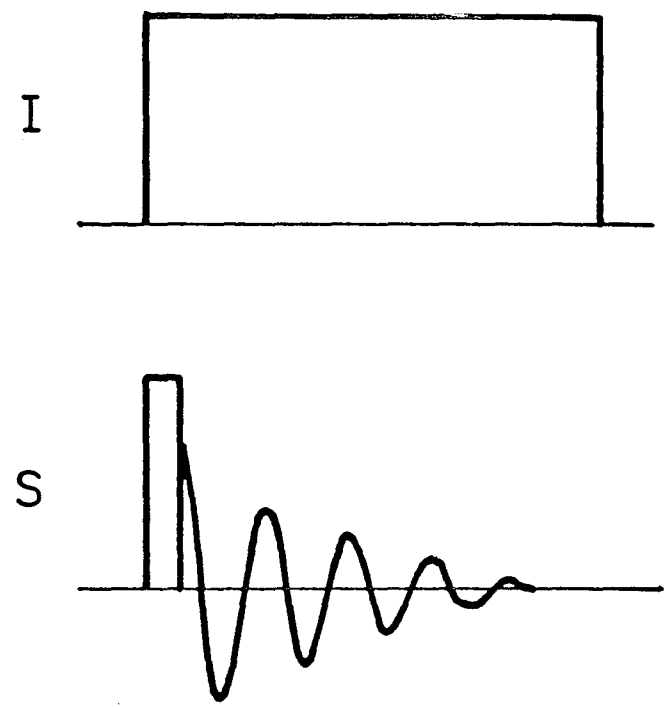

XBL758-6988

Figure 1

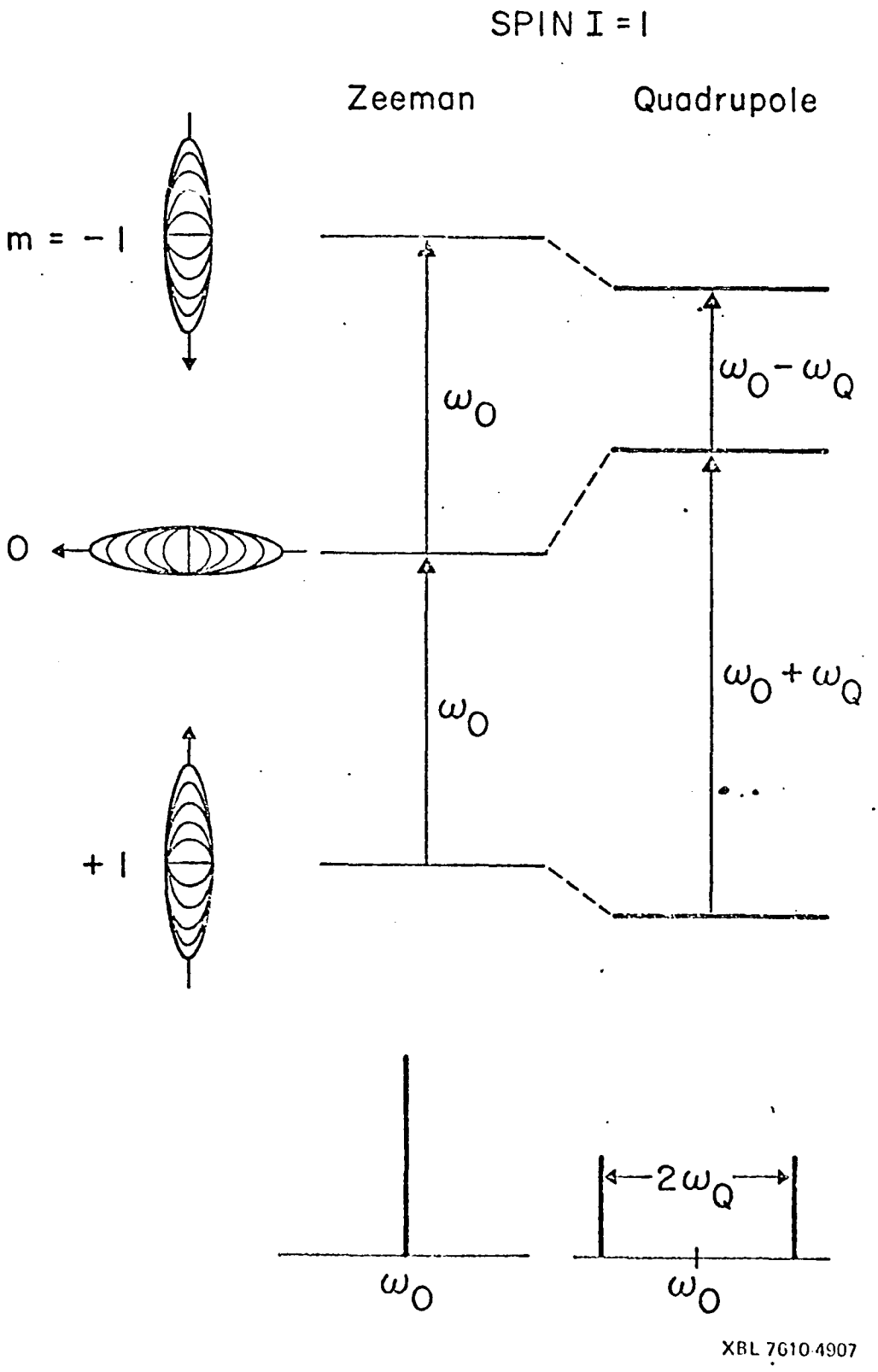
SPIN I = 1
Zeeman
Quadrupole
m = −1
0
+1
ω_0
ω_0
$\omega_0 - \omega_Q$
$\omega_0 + \omega_Q$
$2\omega_Q$
ω_0
ω_0
XBL 7610-4907

Figure 2

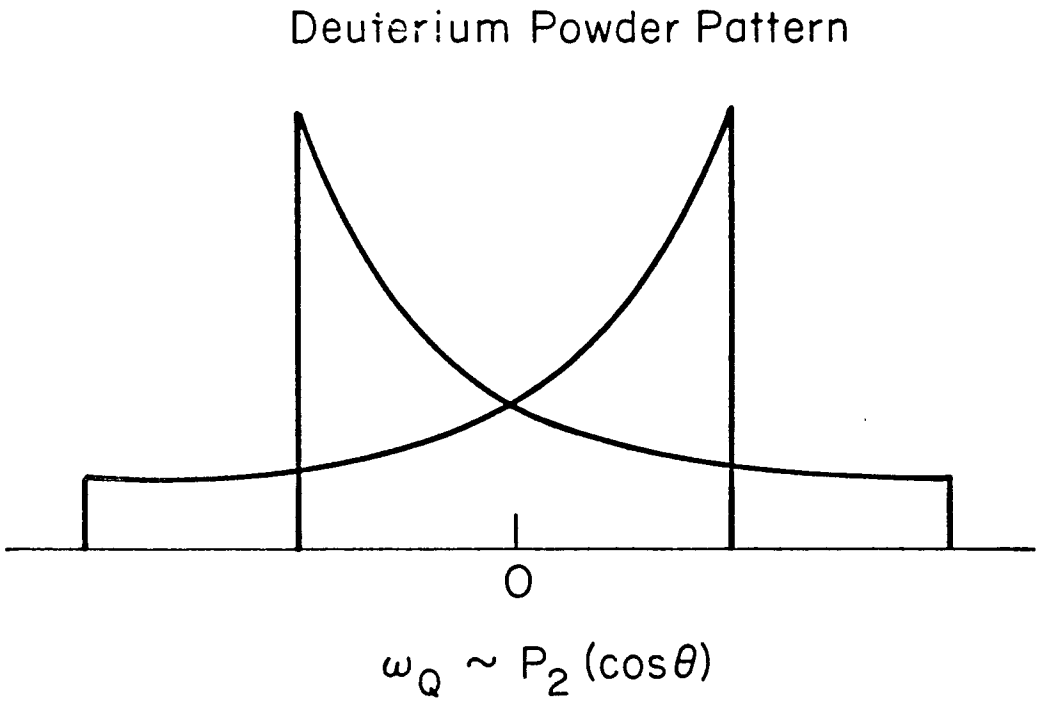

XBL 7610-4908

Figure 3

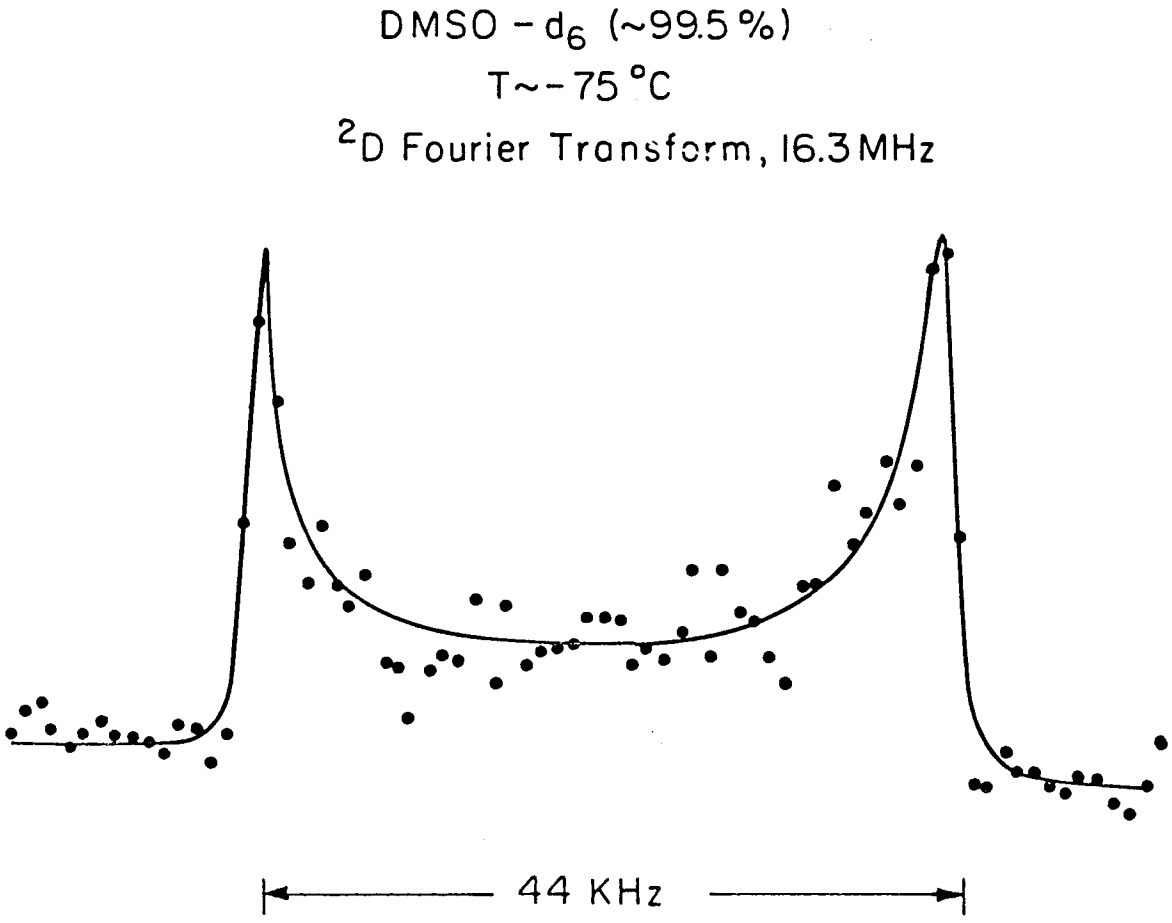
DMSO - d_6 (~99.5 %)
T~-75 °C
^{2}D Fourier Transform, 16.3 MHz
44 KHz
XBL756-6464

Figure 4

Deuterium Decoupling

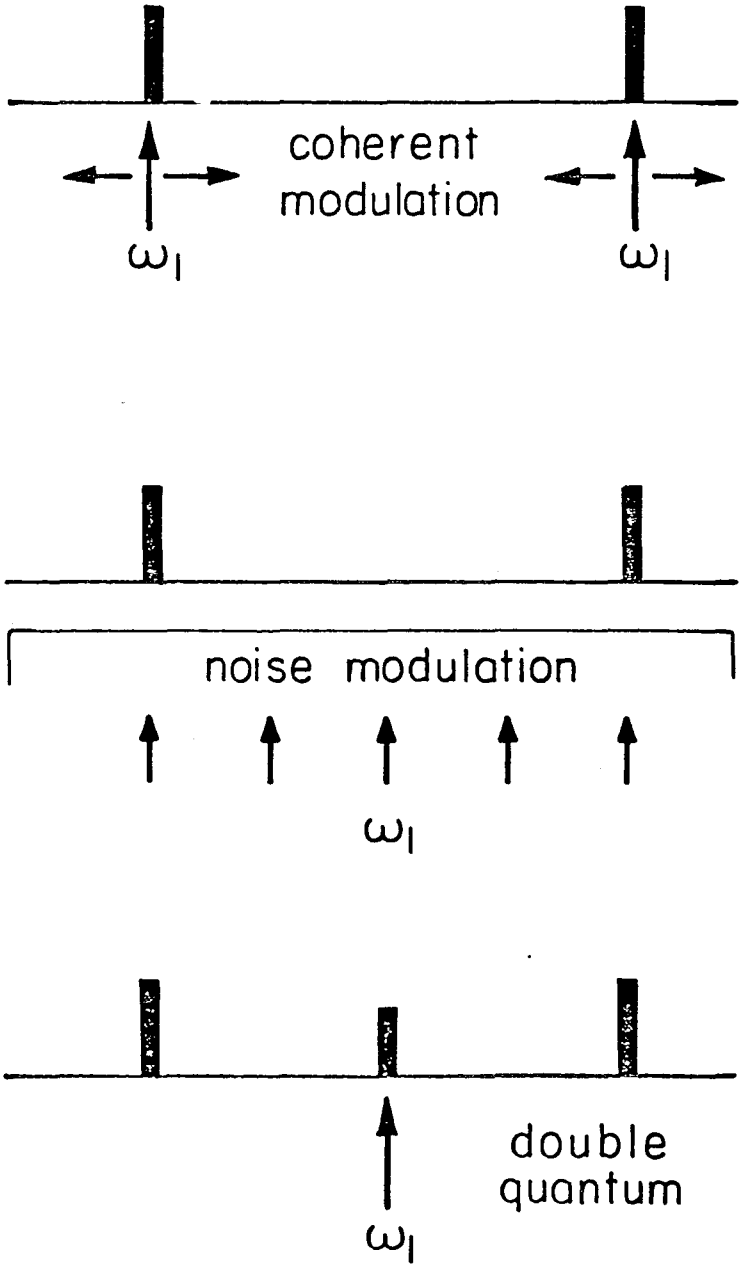

Figure 5

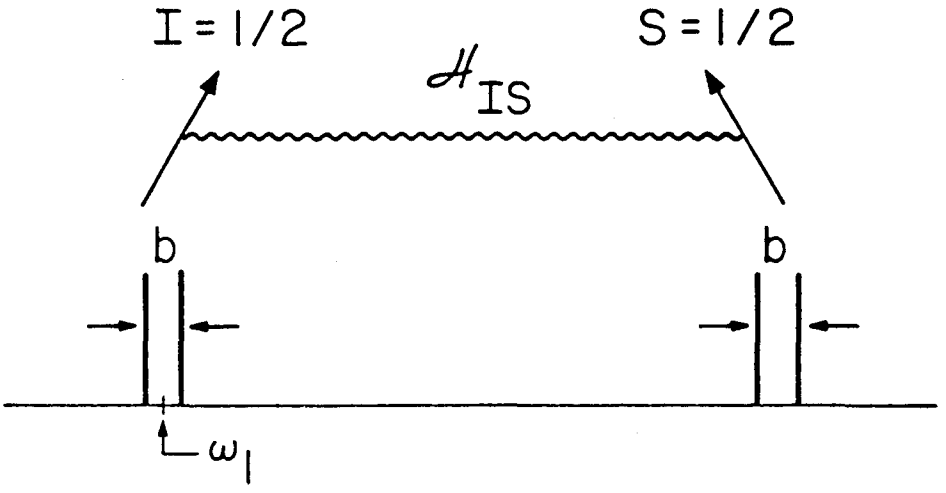

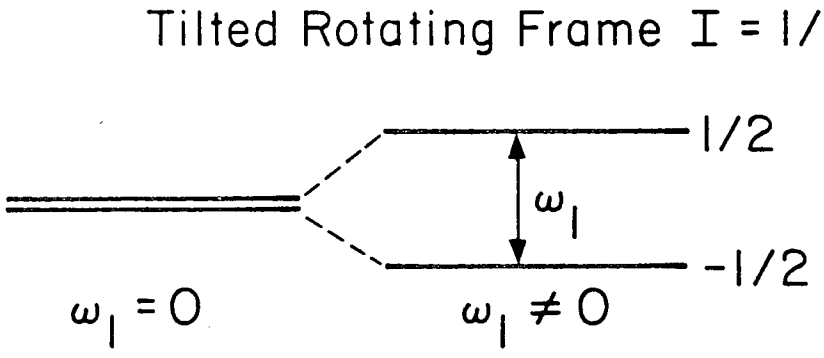

XBL 764-1520

Figure 6

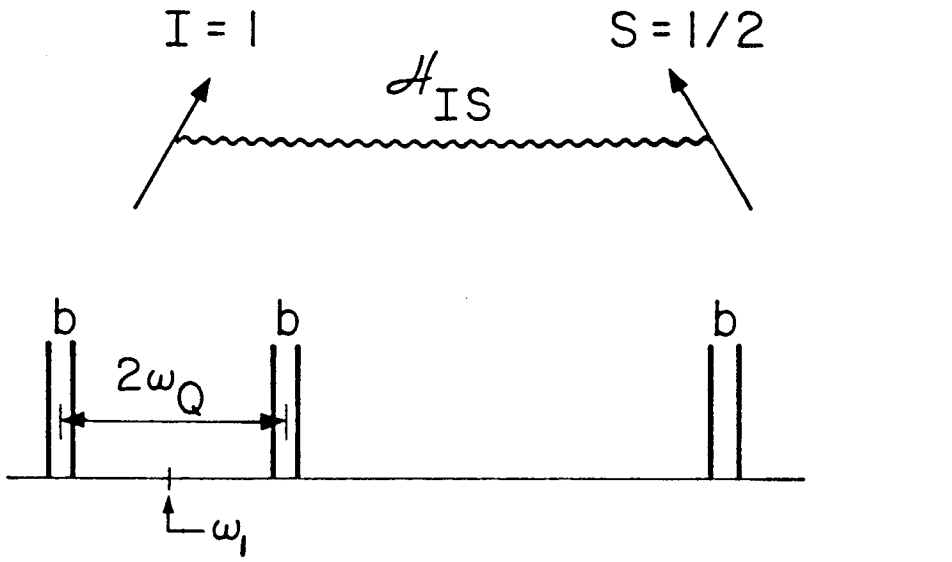

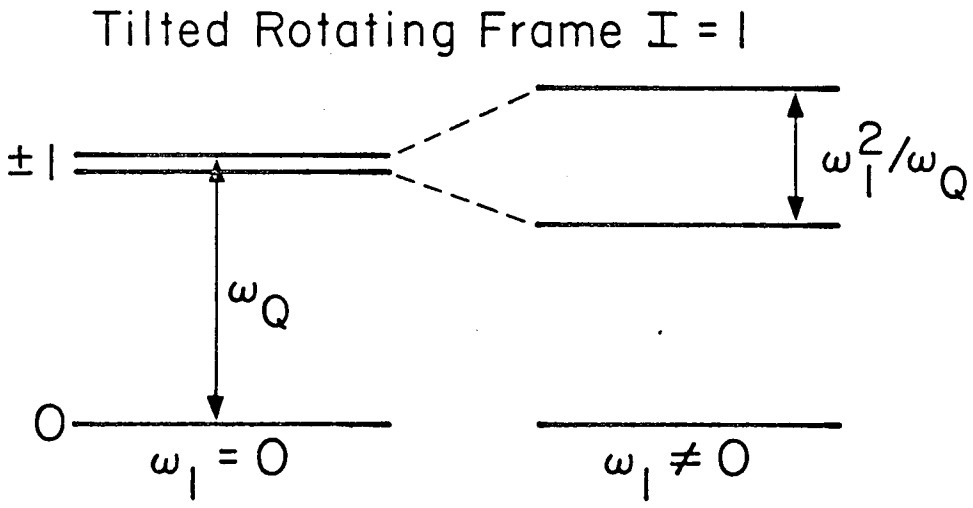

XBL 764-1506

Figure 7

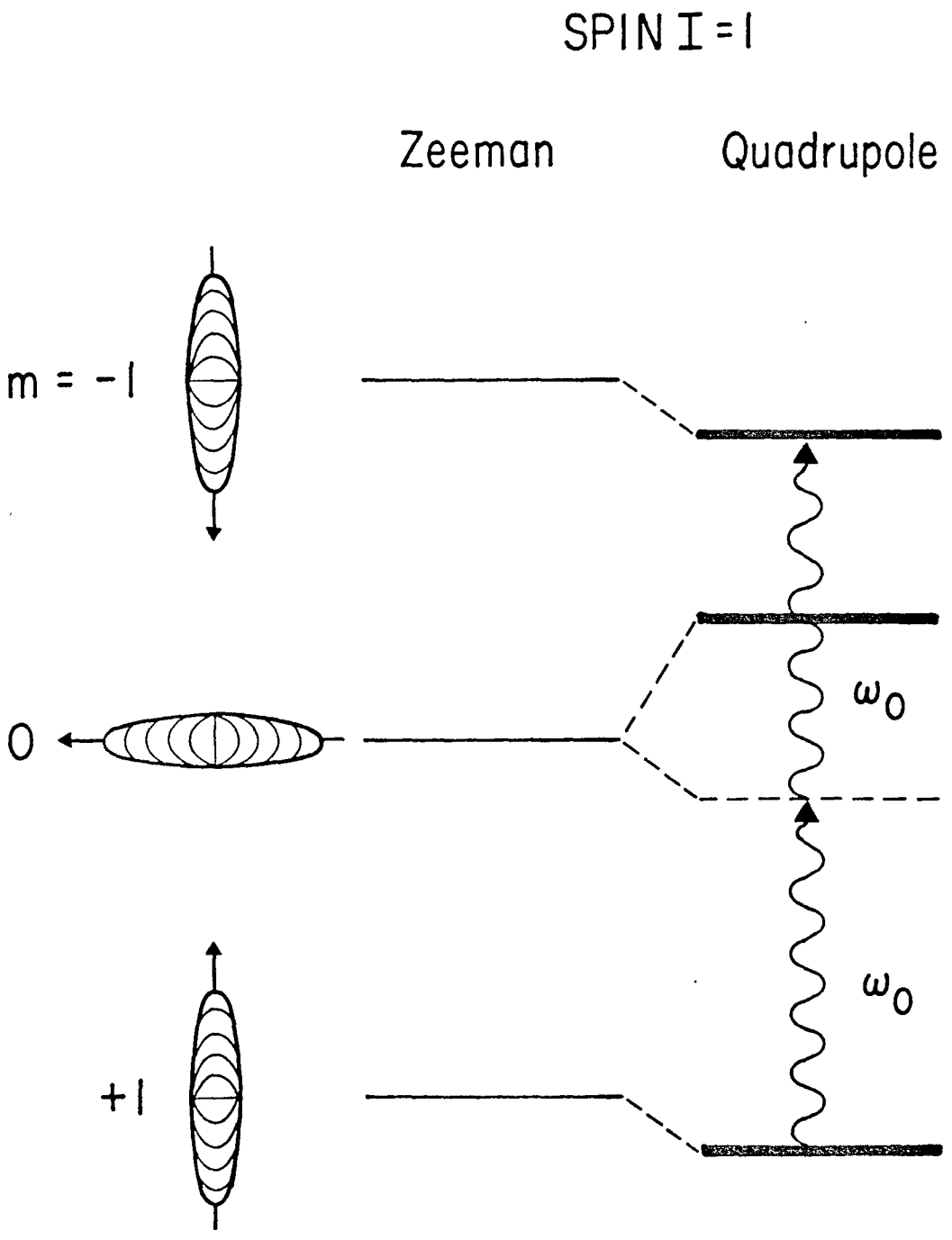

Figure 8

z-Frame Double-Quantum
Effective Fields

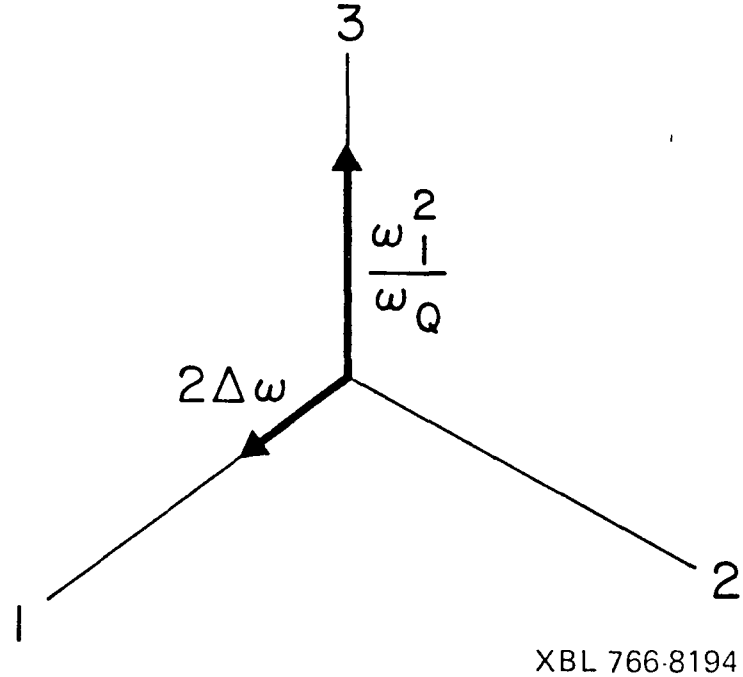

XBL 766-8194

Figure 9

Deuterium Decoupling
($\omega_Q \gg D$)

Single Quantum, on resonance

$$\omega_1^2 \gtrsim D^2$$

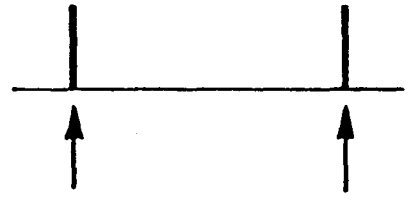

Single Quantum, off resonance by ω_Q

$$\omega_1^2 \gtrsim \omega_Q^2$$

Double Quantum, on resonance

$$\omega_1^2 \gtrsim D\omega_Q$$

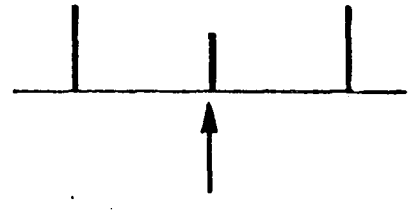

XBL756-6458A

Figure 10

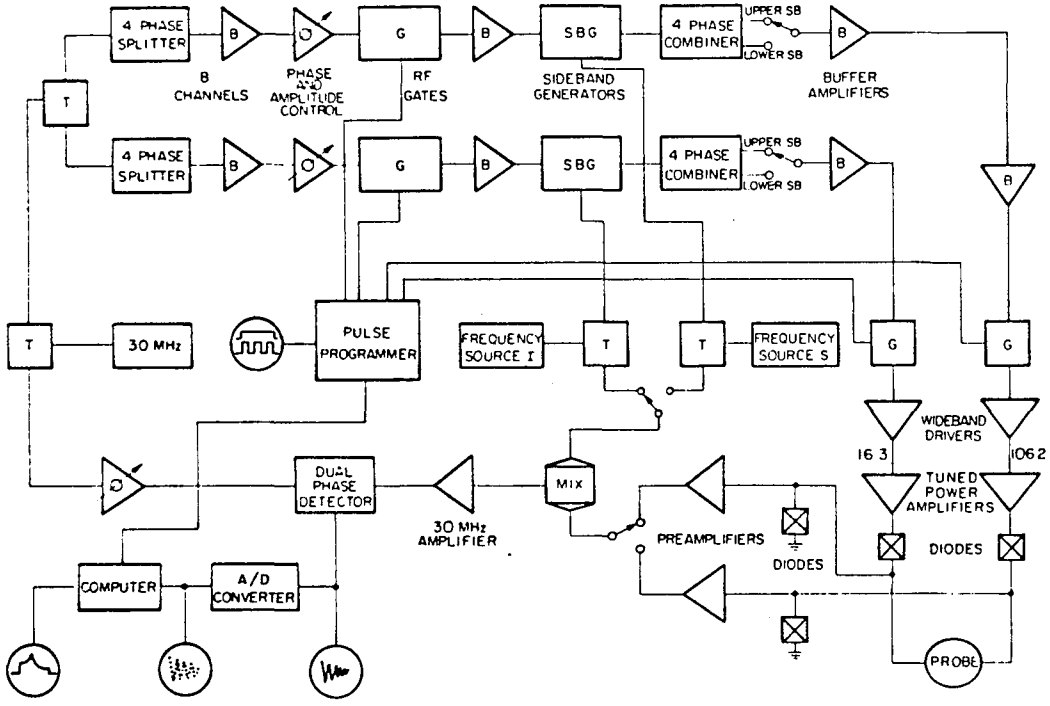

Figure 11

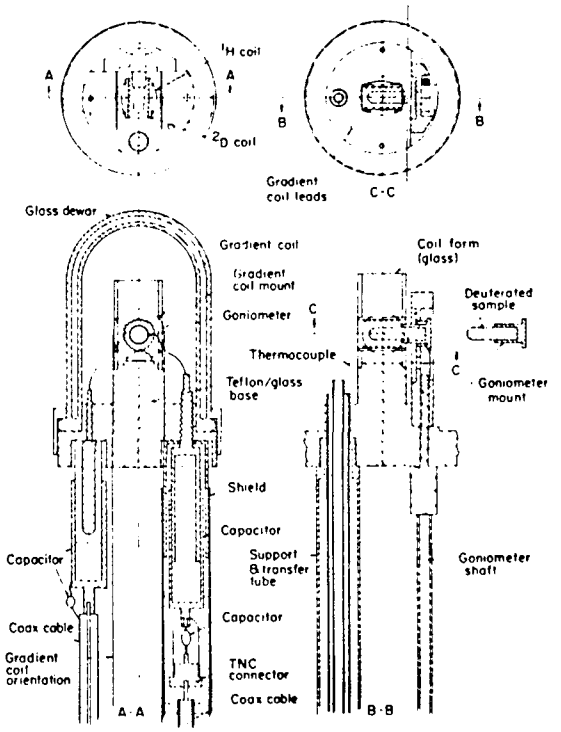

XBL 766-1989

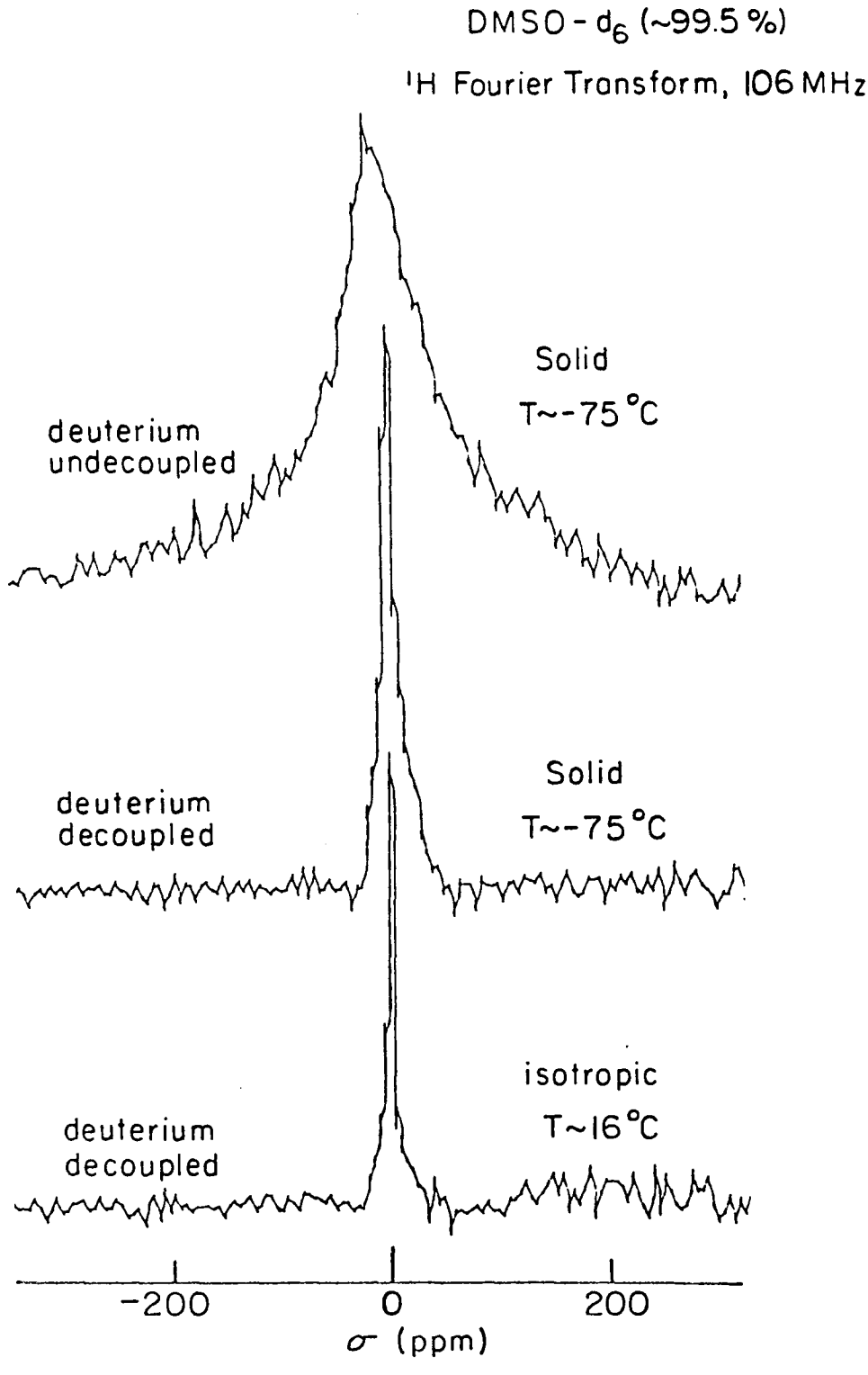
DMSO - d_6 (~99.5 %)
^{1}H Fourier Transform, 106 MHz
deuterium undecoupled
Solid
T~-75 °C
deuterium decoupled
Solid
T~-75 °C
deuterium decoupled
isotropic
T~16 °C
-200
0
200
σ (ppm)
XBL756-6467

Figure 12

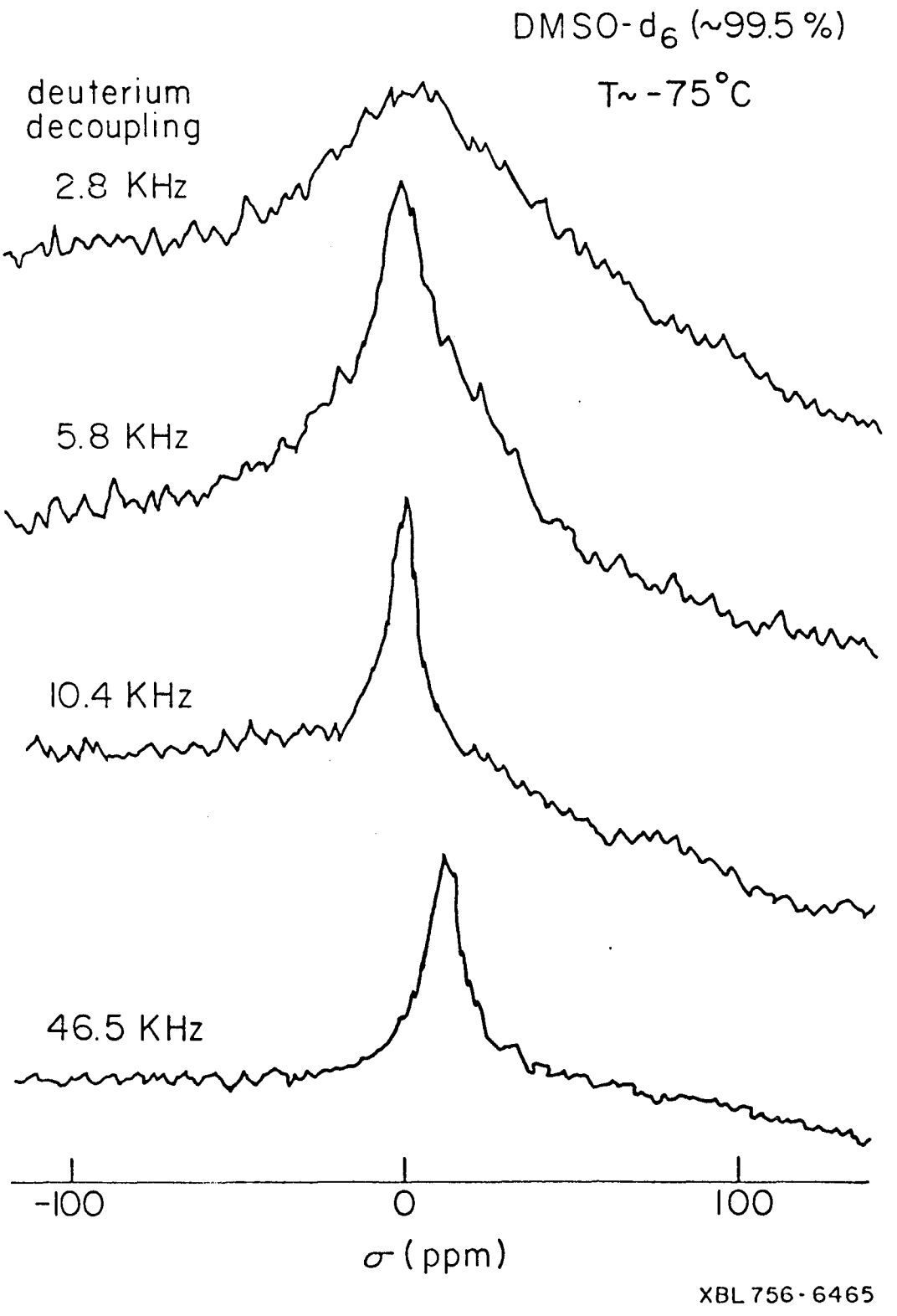
DMSO-d_6 (~99.5 %)
T~ -75°C
deuterium decoupling
2.8 KHz
5.8 KHz
10.4 KHz
46.5 KHz
-100
0
100
σ (ppm)
XBL 756-6465

Figure 13

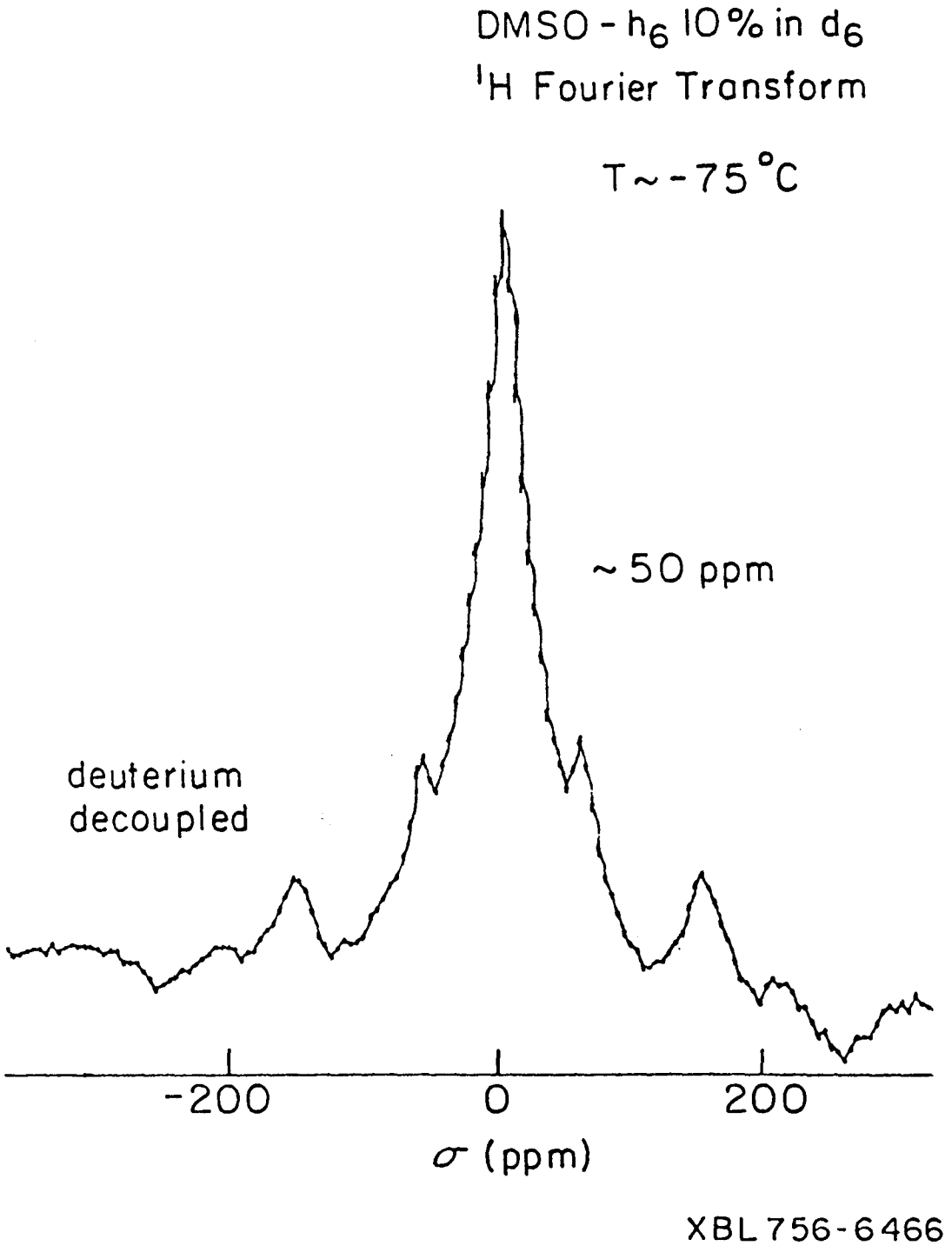
DMSO - h_6 10% in d_6
^{1}H Fourier Transform
T ~ -75 °C
~ 50 ppm
deuterium
decoupled
-200
0
200
σ (ppm)
XBL 756-6466

Figure 14

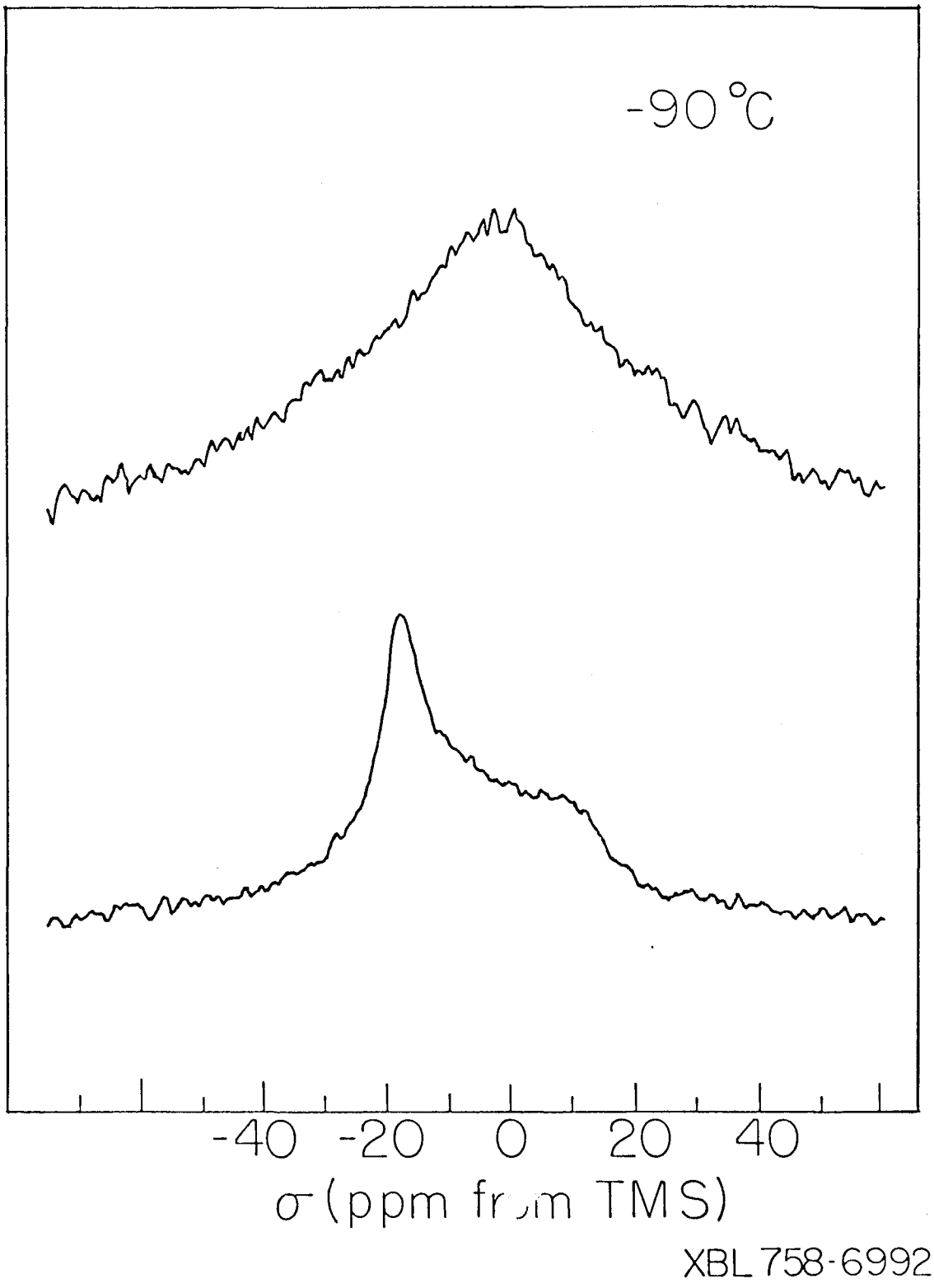

Figure 15

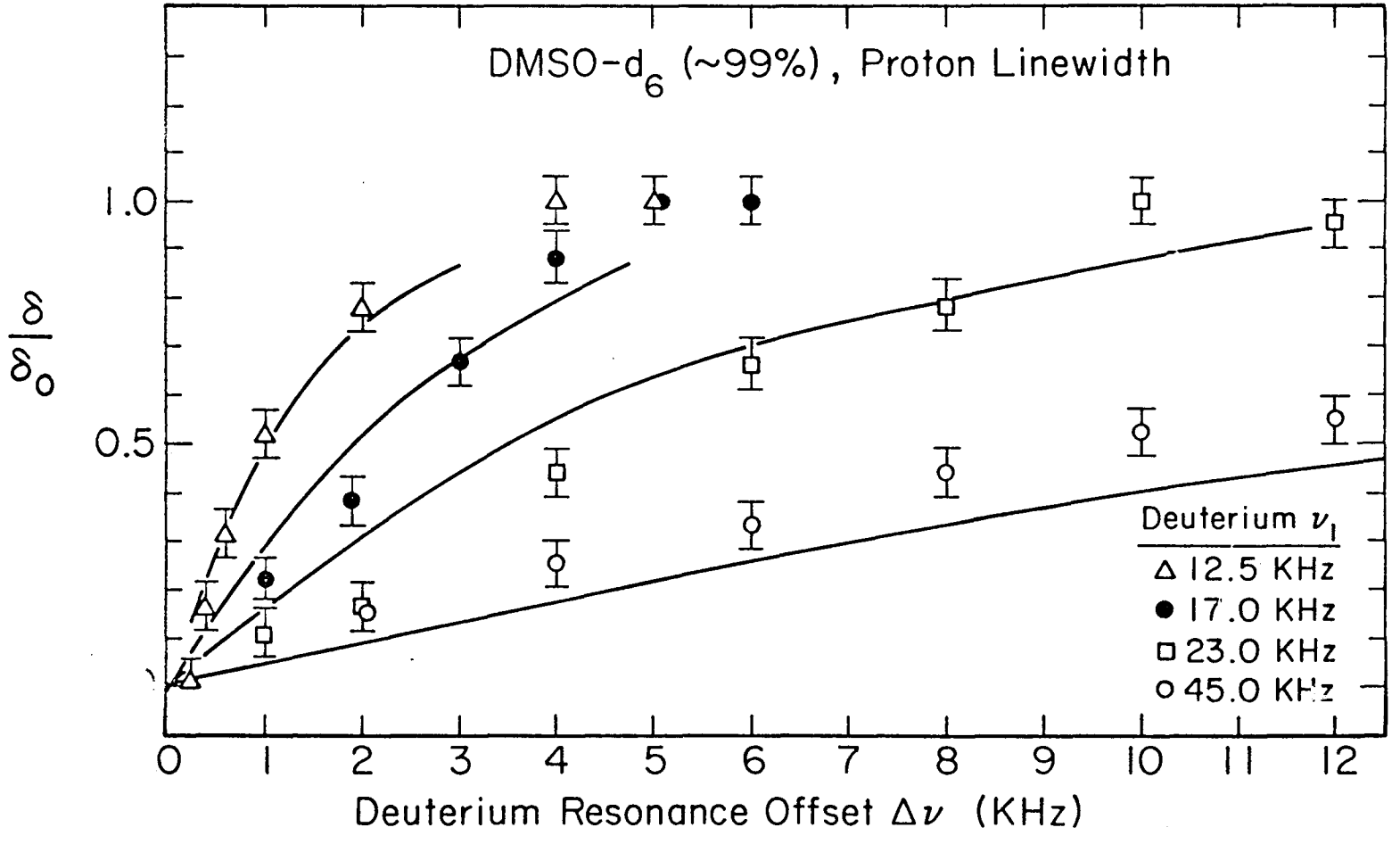

XBL 764-1504 A

Figure 16

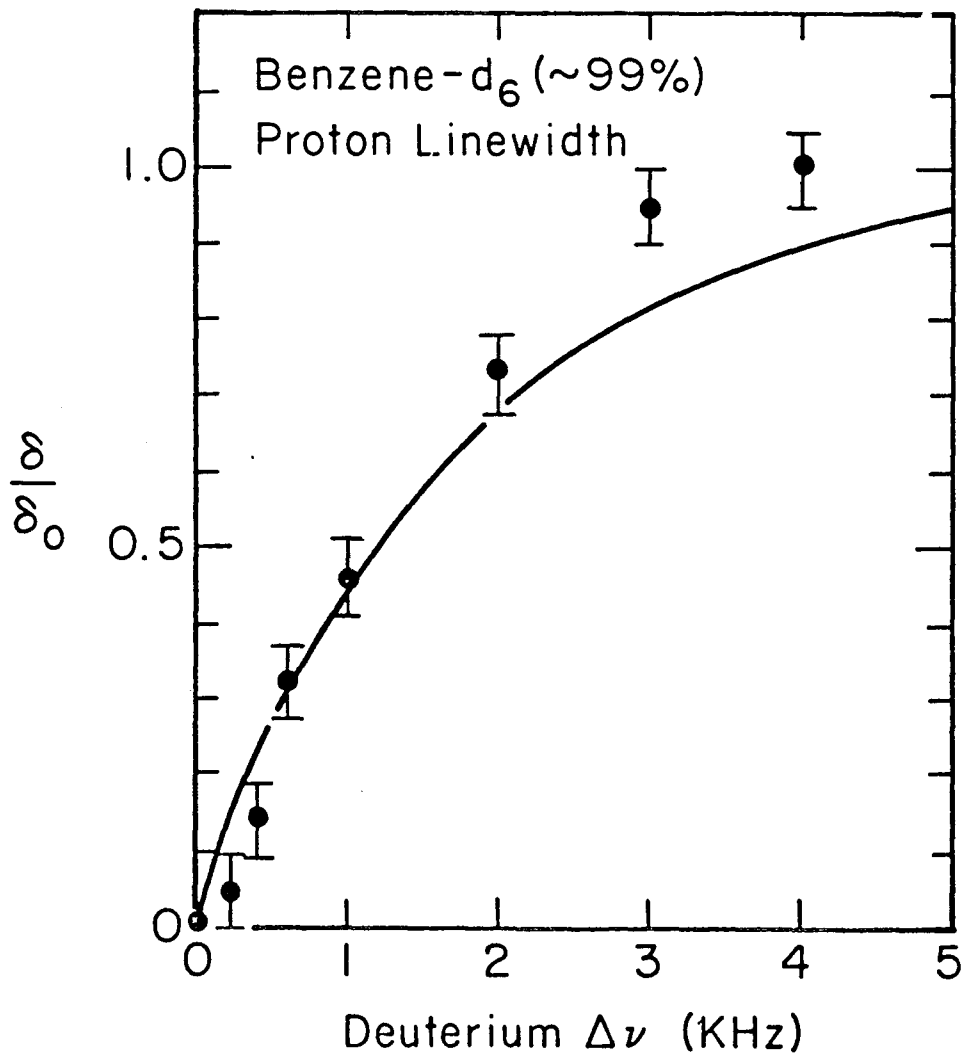

XBL 764-1519 a

Figure 17

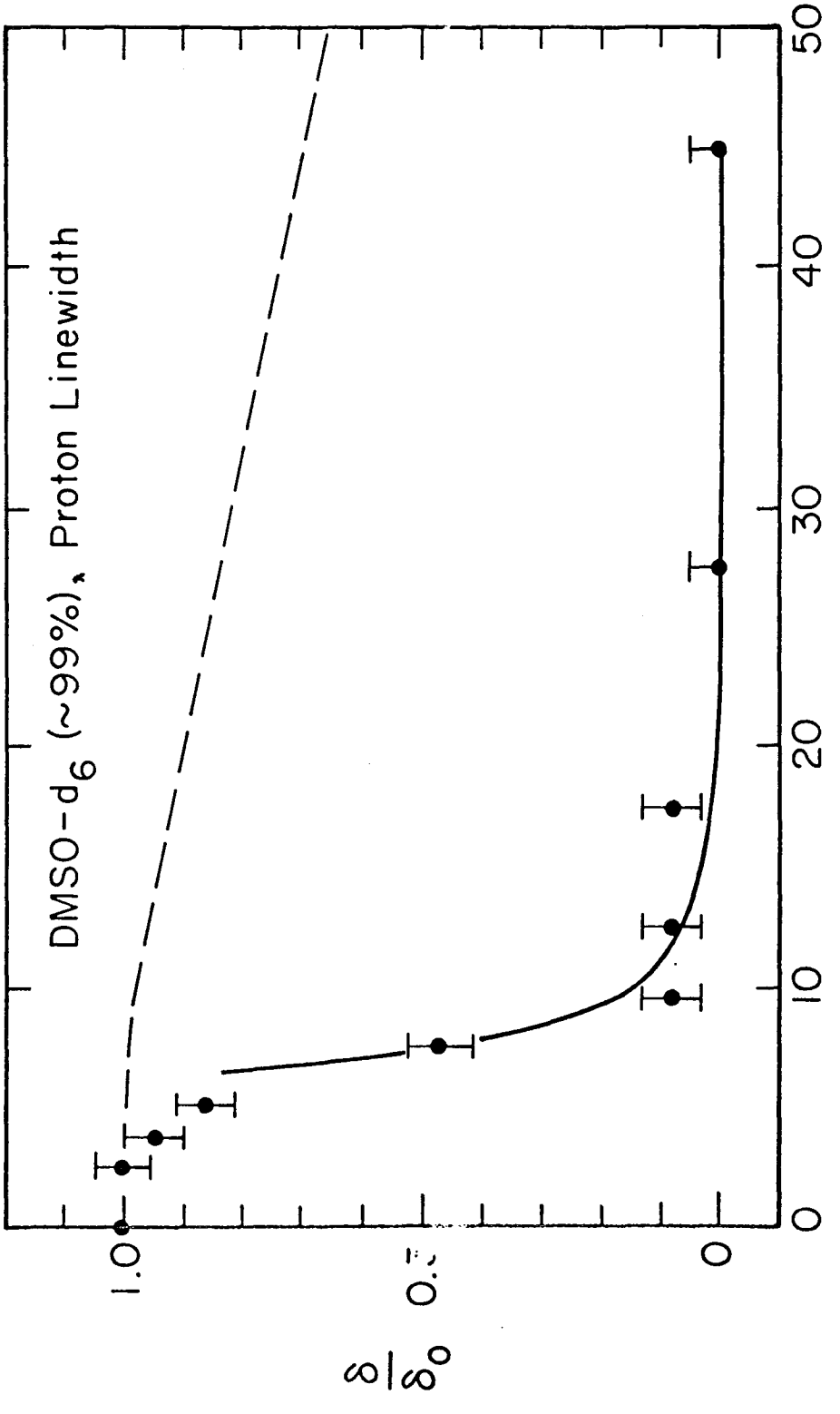
DMSO-d_6 (~99%), Proton Linewidth
Deuterium ν_1 (KHz)
δ/δ^o
1.0
0.5
0
0
10
20
30
40
50
XBL 764-1523A

Figure 18

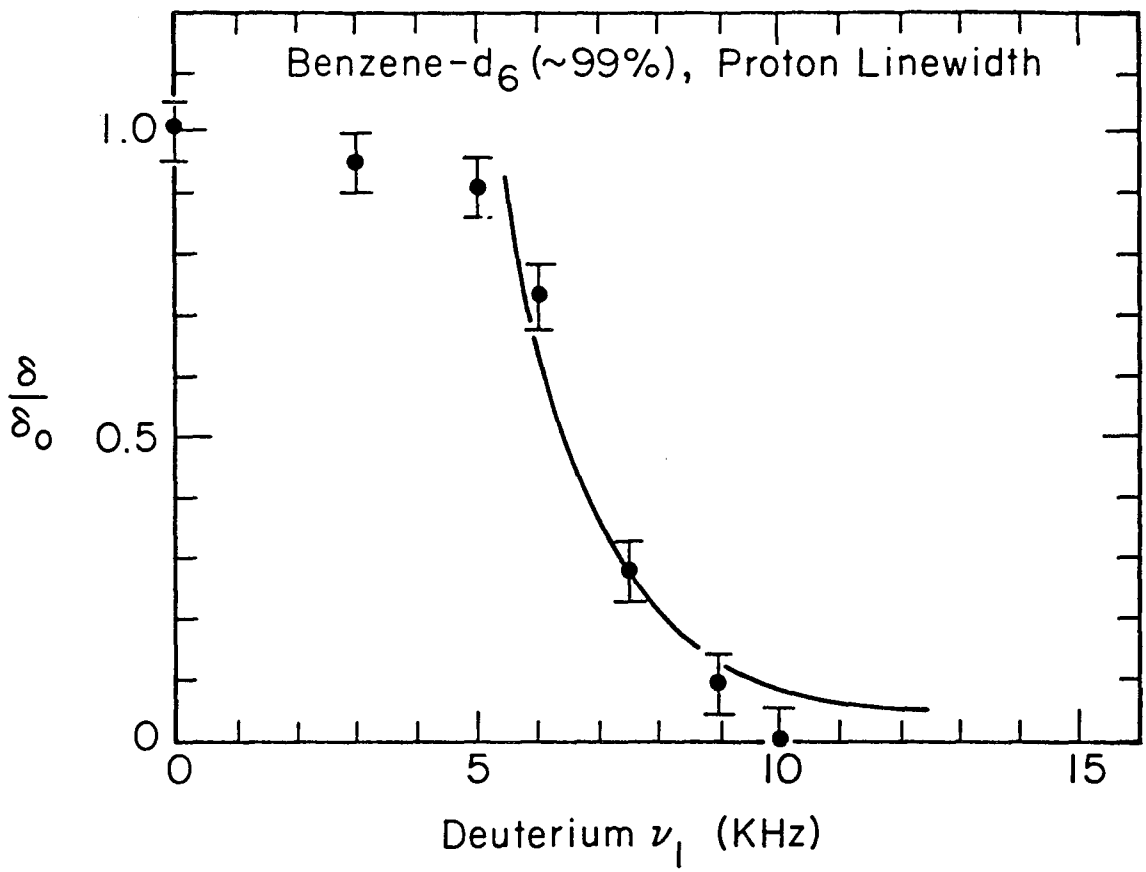

XBL 764-1518a

Figure 19

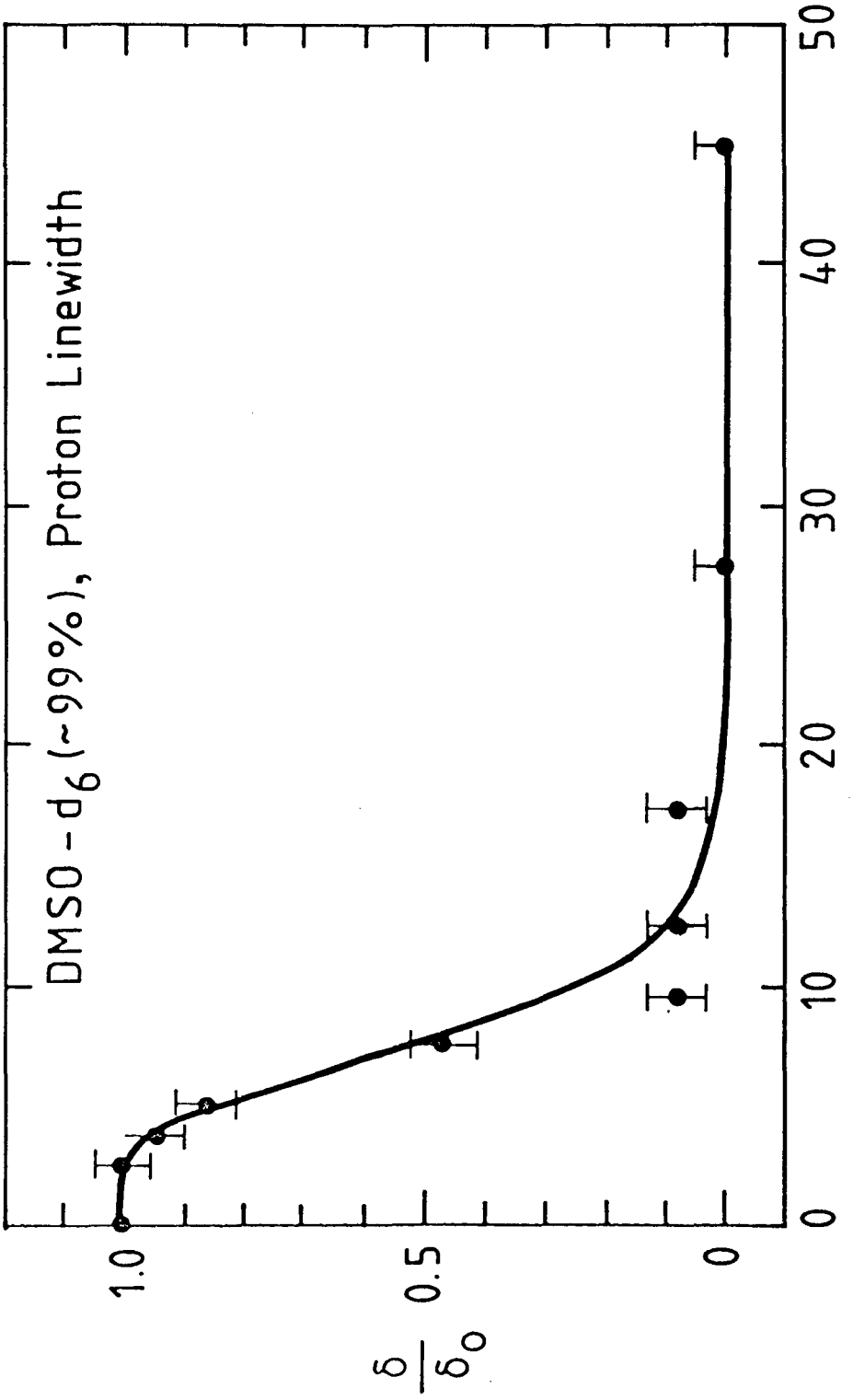
DMSO-d_6 (~99%), Proton Linewidth
δ/δ_o
1.0
0.5
0
0
10
20
30
40
50
Deuterium ν_1 (KHz)
XBL 7710-10314

Figure 20

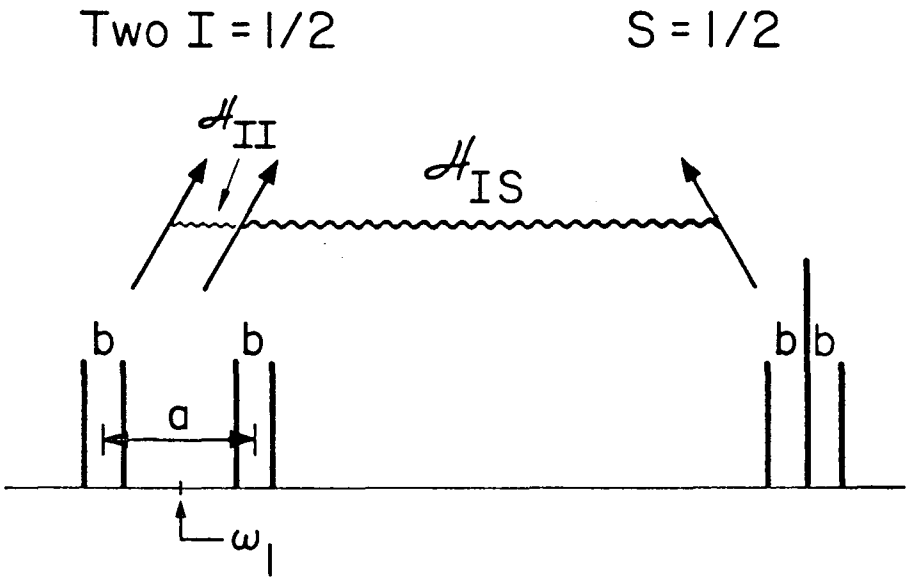

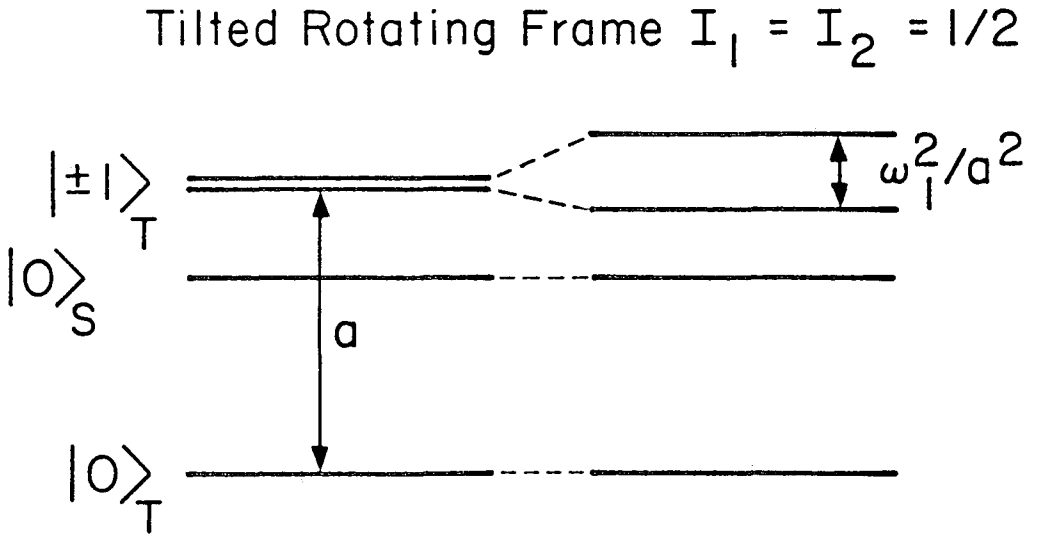

XBL 764-1521 A

Figure 21

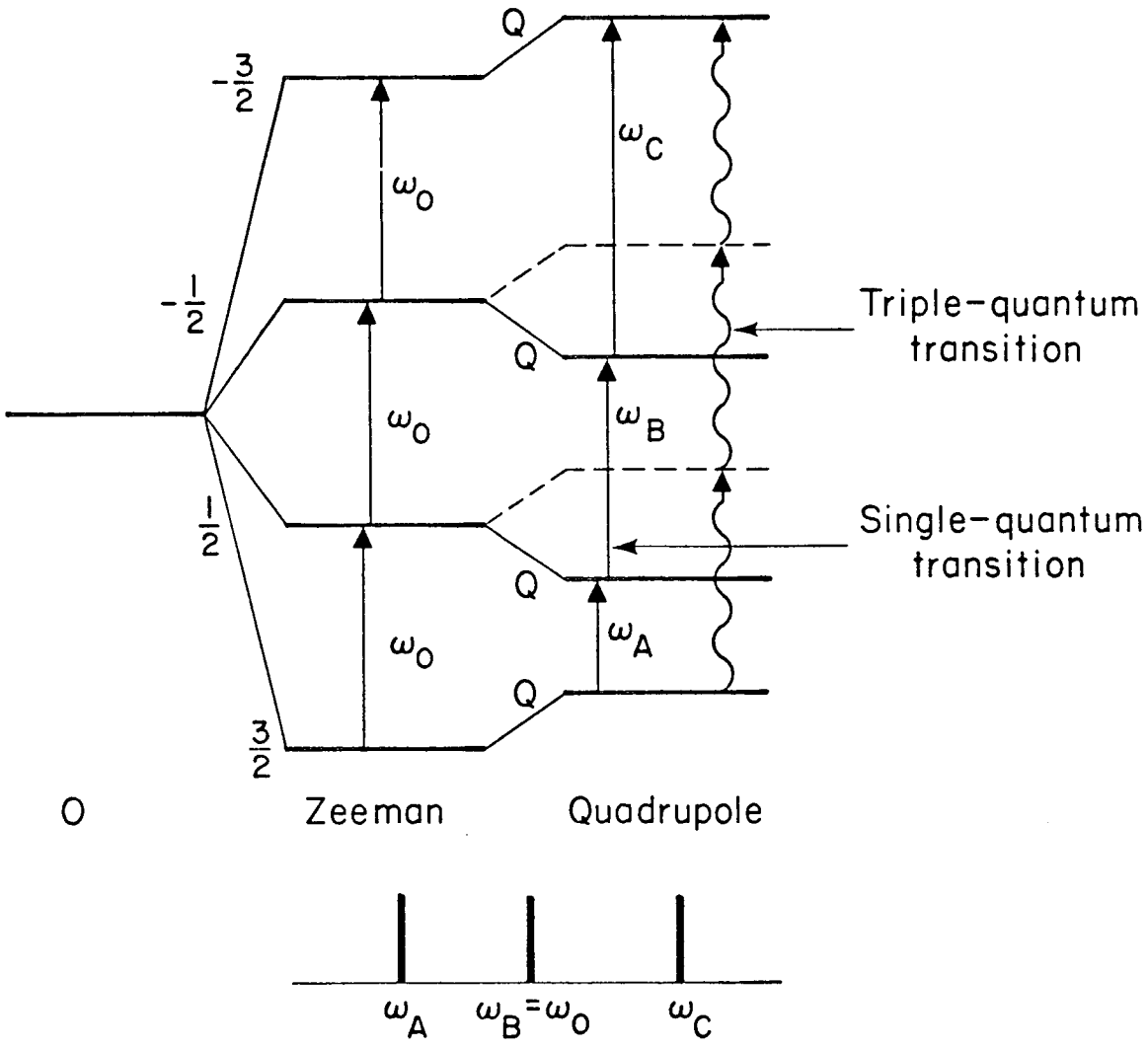

XBL 764-1278

Figure 22

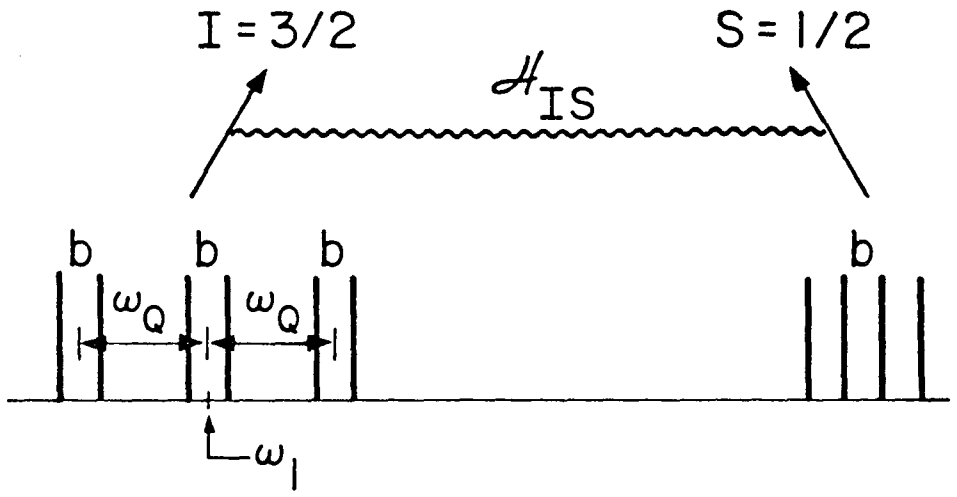

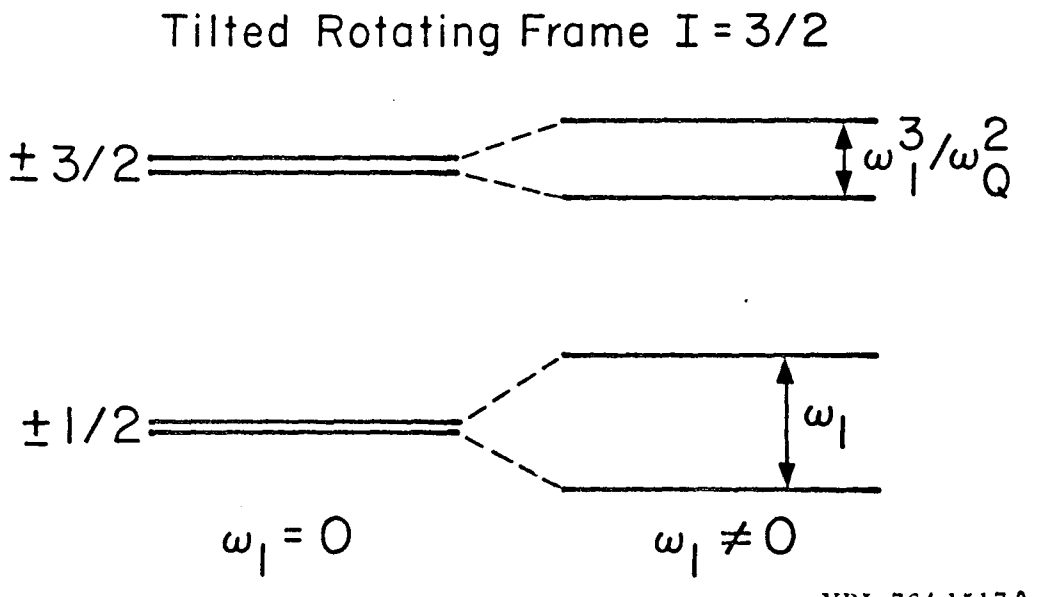

XBL 764-1517A

Figure 23

This report was done with support from the Department of Energy. Any conclusions or opinions expressed in this report represent solely those of the author(s) and not necessarily those of The Regents of the University of California, the Lawrence Berkeley Laboratory or the Department of Energy.

TECHNICAL INFORMATION DEPARTMENT
LAWRENCE BERKELEY LABORATORY
UNIVERSITY OF CALIFORNIA
BERKELEY, CALIFORNIA 94720